ESC European Society of Cardiology

Cardiovascular Research (2025) **121**, 1187–1203
https://doi.org/10.1093/cvr/cvaf077

Proteomic profiling reveals a higher presence of glycolytic enzymes in human atherosclerotic lesions with unfavourable histological characteristics

Kaylin C.A. Palm [1], Xiaoke Yin [2], Ferheen Baig[3], Konstantinos Theofilatos [3], Sander W. van der Laan[1,4], Gert J. de Borst [5], Dominique P.V. de Kleijn[5], Johann Wojta [6], Stefan Stojkovic[6], Manuel Mayr[2,6], Hester M. den Ruijter [7], Gerard Pasterkamp [1], Ernest Diez Benavente [7†], and Michal Mokry [1,7*†]

[1]Division Laboratories, Pharmacy, and Biomedical Genetics, Central Diagnostics Laboratory, University Medical Centre Utrecht, Heidelberglaan 100, 3584 CX, Utrecht, The Netherlands; [2]National Heart and Lung Institute, Imperial College London, Dovehouse St, London SW36LY, UK; [3]King's British Heart Foundation Centre, Kings College London, Strand, London WC2R2LS, UK; [4]Centre of Population Health and Genomics, University of Virginia, 1335 Lee St, Charlottesville, 22908 VA, USA; [5]Division of Surgical Specialties, Department of Vascular Surgery, University Medical Centre Utrecht, Utrecht University, Heidelberglaan 100, 3584 CX, Utrecht, The Netherlands; [6]Division of Cardiology, Department of Internal Medicine II, Medical University of Vienna, Spitalgasse 23, 1090 Wien, Austria; and [7]Division of Heart and Lungs, Laboratory of Experimental Cardiology, University Medical Centre Utrecht, Utrecht University, Heidelberglaan 100, 3584 CX, Utrecht, The Netherlands

Received 7 October 2024; revised 18 February 2025; accepted 16 March 2025; online publish-ahead-of-print 12 May 2025

Time of primary review: 59 days
See the editorial comment for this article 'Deciphering metabolic reprogramming in atherosclerosis through a multi-omics approach', by P. Azar and M.-L. Bochaton-Piallat, https://doi.org/10.1093/cvr/cvaf114.

Aims

Molecular characterization of vulnerable atherosclerotic plaques often relies on transcriptomic data. However, RNA expression may not consistently align with protein expression. The proteomic landscape linked to plaque vulnerability is underexplored in human lesions. In this study, we analyzed a large mass spectrometry-based proteomics dataset from the plaque tissue of 320 patients to identify the molecular mechanisms associated with vulnerable plaques. Previous studies have shown significant differences in cell metabolism in murine atherosclerosis models, prompting an in-depth description of expression of key enzymes in glycolysis in human atherosclerotic plaques.

Methods and results

Atherosclerotic lesions from 320 patients undergoing carotid endarterectomy surgery were collected (200 discovery set and 120 for the validation set) and underwent proteomic analyses. Plaque samples were digested, enriched for extracellular matrix proteins, and processed for untargeted proteomics analysis. The resulting protein levels were linked to pathological plaque characteristics, bulk and single cell transcriptomics, and clinical data. Proteomic analysis of 200 human atherosclerotic carotid lesions detected 1499 proteins with most showing poor correlation with RNA levels. We identified 240 proteins associated with plaque vulnerability index ($FDR < 0.05$), including key glycolysis enzymes: Hexokinase 3 (HK3) ($P = 0.003$, $FDR = 0.03$), PKM ($P = 0.008$, $FDR = 0.05$), and LDHA ($P = 0.006$, $FDR = 0.04$). The observed associations were mainly driven by macrophage content and fat content, reflected the severity of pre-operative symptoms, exhibited significant sex differences, and correlated with plaque haemorrhage biomarker BLVRB. Validation in 120 patients confirmed HK3 and PKM's association with plaque progression and clinical symptoms (all $P < 0.001$).

Conclusion

Enzymes involved in the glycolysis process are more abundant in plaques with vulnerable histological characteristics and are significantly associated with plaque haemorrhage biomarker BLVRB. This implies that plaque destabilisation may be driven by higher glycolysis metabolism, which may contribute to plaque haemorrhage. This association was stronger in women, underlining the important role of energy metabolism in sex-specific mechanisms of atherosclerotic disease.

Keywords Atherosclerosis • Proteomics • Glycolysis • Metabolism • Multi-omics • Cardiovascular disease

---

* Corresponding author. Tel: +31 (0)88 75 57770, E-mail: m.mokry@umcutrecht.nl
† Shared.

1. Introduction

Atherosclerosis, a chronic disease of the arteries, is a major contributor to worldwide morbidity and mortality.[1] Advanced atherosclerotic plaques are commonly categorized in two main types of lesions: stable solid fibrous lesion and vulnerable lipid-rich thin capped inflammatory lesions.[2] In recent years, histological and multi-omics studies utilized the analysis of cell structure, ultrastructure of the matrix components, and the histochemical composition of the lesion to identify mechanisms that are relevant for plaque progression and destabilisation.[3,4] The histological composition of human plaques is associated with clinical manifestations of atherosclerotic disease.[5,6] Molecular mechanisms behind the different pathological features are less understood and have mostly been studied extensively in animal studies.[7] Furthermore, supportive evidence from human studies is often limited to immunohistochemical staining to understand spatial relevance of a protein of interest. However, with the increasing availability of more affordable sequencing platforms, the number of reports on single cell and bulk transcriptomic analyses of human atherosclerotic lesions has risen significantly.[8–11] Despite this, previous studies have reported that gene and protein expression are poorly correlated.[12,13]

The search for the proteomic architecture linked with vulnerable pathological phenotypes remains relatively unexplored in human atherosclerotic lesions. We hypothesized that the proteomic analysis of atherosclerotic lesions of many patients would expose potential mechanistic pathways that play a role in plaque destabilisation. Therefore, we analysed a large mass spectrometry-based proteomics dataset from human plaque tissue of 320 patients (200 discovery and 120 validation) and integrated it with clinical, histological, bulk and single cells transcriptomics to unravel the molecular mechanisms linked to vulnerable plaques. We highlight the increased presence of key enzymes involved in glycolysis in vulnerable plaques, which exhibit destabilising features such as high macrophage content and atheromatous tissue.

2. Methods

2.1 Study design

A selection of atherosclerotic plaque samples in this study were retrieved from the Athero-Express biobank, an ongoing study that collects plaque tissue, blood, and extensive clinical data, from patients undergoing carotid endarterectomy (CEA) surgery.[14] A total of 200 plaques samples were selected with the highest possible overlap with existing bulk RNAseq, bulk methylation, histological, and GWAS data. Additionally, we ensured that this subset was representative of the broader Athero-Express carotid cohort by maintaining comparable distributions of age, sex, diabetes status, smoking status, and plaque characteristics. Clinical data was retrieved from patient files and through standardized questionnaires. The indication for a CEA was based on recommendations from the Asymptomatic Carotid Surgery Trial for asymptomatic patients and the European Carotid Surgery Trial and the North American Symptomatic Carotid Endarterectomy Trial for symptomatic patients.[15] Indications for CEA were evaluated by a multidisciplinary vascular team.[14] The removal of atherosclerotic plaques was performed by a team of experienced surgeons, and standardized treatment protocols were applied. All patients were examined by a neurologist for assessment of their preoperative neurologic status. The performed study is in line with the Declaration of Helsinki, and informed consent was provided by all study participants after approval for this study by the medical ethical committees of the respective hospitals (University Medical Centre, Utrecht, The Netherlands, and St. Antonius Hospital, Nieuwegein, The Netherlands) was obtained.

2.2 Histology examination

All CEA plaque samples were histologically examined as described before.[5] According to a standardized protocol, the human carotid artery plaque was divided in segments of 5-mm thickness along the longitudinal axis. The segment with the greatest plaque burden was subjected to histological examination. Semi-quantitative estimation of the plaque morphology was performed for macrophage infiltration (CD68), smooth muscle cell (SMC) content (α-actin), amount of collagen (picrosirius red), and calcification (haematoxylin and eosin). Histological plaque characteristics were scored as (i) no or minor staining or (ii) moderate or heavy staining of macrophages, SMCs, and collagen content. The criteria for classification were defined as follows: for macrophages: (i) absent or minor CD68 staining with negative or clusters with <10 cells present; (ii) moderate or heavy staining, cell clusters with >10 cells present or abundance of positive cells; for SMCs: (i) no or minor α-actin staining over the entire circumference with absent staining at parts of the circumference of the arterial wall; (ii) positive cells along the circumference of the luminal border, with locally at least few scattering cells; for collagen staining: (i) no or minor staining along part of the luminal border of the plaque; (ii) moderate or heavy staining along the entire luminal border; and for calcification: (i) no or minor staining along part of the luminal border of the plaque or a few scattered spots within the lesion; (ii) moderate or heavy staining along the entire luminal border or evident parts within the lesion. In addition, macrophage infiltration and SMC content were scored as the percentage of the total plaque area with the specific staining by using computerized analyses to validate the semi-quantitative analyses. Plaque haemorrhage was defined as the composite of plaque bleeding at the luminal side of the plaque as a result of plaque disruption and intraplaque haemorrhage, which is observed as a haemorrhage within the tissue of the plaque.[16,17] Plaque haemorrhage was examined with haematoxylin, eosin, and fibrin stainings and rated as being absent or present.[16,17] Using CEA plaques samples from the Athero-Express biobank the presence of plaque Hexokinase 3 (HK3) expression was assessed using rabbit polyclonal anti-human HK3 (1/1000, Atlas Antibodies, Cat#HPA056743 RRID:AB_2683222) as described previously by Ménégaut *et al.*[18] Presumed artefacts of surgery such as accumulation of erythrocytes along the border of the specimen were not included in the definition of plaque haemorrhage. Intraplaque vessels were stained with CD34 antibody. Plaque vessel density was determined by the average number of vessels of 3 to 4 hot spots within every single plaque, with increased vessel density defined as an average vessel count per hot spot higher than the median (=8) of the cohort. Overall plaque phenotype was determined using Picrosirius red with polarized light and haematoxylin stains to assess the percentage of atheroma of the total area of the plaque, which resulting in three groups: fibrous plaques containing <10% fat; fibro-atheromatous, 10 to 40%; or atheromatous, > 40% fat.[14] Plaque vulnerability was assessed using plaque vulnerability index (PVI), a variable previously described before,[14] which is a semi-quantitative score that summarizes the presence of various plaque characteristics associated with plaque instability, such as heavy/moderate macrophage, no/minor collagen, no/minor SMC, moderate/heavy calcification, and moderate/heavy fat content. A score of 1 is given for each of these when present in the plaque. While, for each plaque characteristic that defines a stable plaque, a score of 0 is added. The summation of the scores results in a final plaque score ranging from 0 (most stable), to 5 (most vulnerable). The histological examinations were performed by two independent observers who were blinded for clinical outcome on a regular basis after processing of the tissue. The histological examination showed good to excellent intra-observer and inter-observer reproducibility on the different items ($\kappa = 0.6$ to 0.9). In addition, the stainings for macrophages and SMCs were scored quantitatively with the use of computer-based analyses. The semi-quantitative and quantitative scorings revealed an excellent correlation. Furthermore, plaque neutrophil levels were assessed by method of immunostaining of CEA plaque segments with mouse anti-human CD66b and MPO antibodies or napthol AS-D chloroacetate esterase. The presence of neutrophils was analysed using image-analysing software and identified by the number of CD66b positive cells expressed as the number of neutrophils per plaque.[19] Similarly, plaque mast cell levels were estimated by method of immunostaining of CEA plaque segments with monoclonal mouse antibody against tryptase and visualized with Liquid Permanent Red. Using Olympus cellSens Dimension 1.15 software mast cells were counted manually and expressed as mast cell/mm^2 plaque size per CEA plaque segment. This method is known to have good intra-observer variability (Spearman's rho = 0.947; $P < 0.001$).[20,21]

2.3 Sample preparation and protein extraction

25–65 mg of human carotid artery cross-section samples from culprit (thickest part of the plaque) specimens were cut into smaller pieces and washed with ice-cold phosphate buffered saline wash solution containing 24 mM EDTA and protease inhibitor cocktail (Sigma Aldrich). To ensure removal of plasma contaminant, the samples were washed three times. Loosely bound proteins were isolated using NaCL extraction buffer (0.5 M NaCl, 25 mM EDTA, 10 mM Tris pH 7.5, plus protease inhibitor) for two hours. The NaCl liquid extract was collected and a NaCl wash was performed on the remaining tissue. After, guanidine hydrochloride buffer (4 M GuHCl, 50 mM sodium acetate pH 5.8 and protease inhibitors) was added to the remaining samples for 72 h to solubilize mature extracellular matrix proteins. 20 µg of Extracted protein was quantified using Pierce BCA protein assay kit (Thermo Scientific). After protein quantification, 20 µg of each GuHCl sample extract was aliquoted into new Eppendorf tubes. Pre-chilled (−20°C) ethanol (10× volume) was used to precipitate the samples overnight at −20°C. Samples were centrifuged at 16 000 × g for 40 min at 0°C and the supernatant subsequently discarded. Protein pellets was dried using a speed vac (Thermo Scientific, Savant SPD131DDA). Dried extracts were frozen at (−20°C) ready for deglycosylation. Then the extract was treated with a 2-step deglycosylation procedure (see Supplementary material online, Methods) before the samples were denatured and reduced with 9 M urea and 3 M thiourea, 100 mM DTT, and 500 mM iodoacetamide. Samples were then precipitated overnight with pre-chilled acetone and the resulting protein pellet were dried using speed vac (Thermo Scientific, Savant SPD131DDA) and then digested with Trypsin/LysC (1:50 protease:protein) overnight at 37°C, 240 rpm. Digestion was halted with the addition of 1% TFA. After further sample purification with Bravo AssayMAP liquid handling system (Agilent) (see Supplementary material online, Methods), the samples were ready for untargeted proteomics analysis.

2.4 Untargeted proteomics and data analysis

Untargeted proteomics analysis was achieved using nanoflow LC system (Dionex Ultimate 3000 RSLC nano) (see Supplementary material online, Methods). 2 µL, 1 µg of protein samples was injected at 0.25 µL/min to separate peptides. Spectra were collected from an Orbitrap mass analyser (Q exactive plus, thermos Fisher Scientific) at a resolution of 60 000 at 200 mass to charge range (m/z). Data-dependent MS2 scan was performed using the top 15 ions in each full MS scan (resolution of 15 000 at 200 m/z) with dynamic exclusion enabled. The generated data was further analysed using thermos scientific proteome discoverer software (version 2.5.0.4.00) and the data was searched against the human database (UniProtKB/Swiss-Prot version from January 2021, 20,396 protein entries) using Mascot (version 2.6.0, Matrix Science). After, ECM and related protein categories were assigned using Matrisome DB (http://matrisomeproject.mit.edu/) and further in-house selection and assignment. Then, protein abundances were normalized based on total protein per sample and scaled using log2 transformation for relative protein quantities. The data was subsequently filtered to only include protein data with <30% missing values. Any remaining missing values within the data were imputed using KNN-Impute method.

2.5 Linear regression models

The proteomics data was tested for significant associations between protein expression (outcome) and multiple histological features (predictors) (see Supplementary material online, PDF *Table S7*) using a linear regression model.

2.6 Bulk and single cell RNA data

RNA expression data was generated as described by Mokry *et al.*[10] from 700 atherosclerotic plaque segments retrieved from the Athero-Express biobank in the study between 2002 and 2016. Differential expression analysis was performed using DESeq2 R package and to correct for multiple testing, Benjamini-Hochberg (BH) adjustment was applied with an FDR < 0.05 considered significant. Plaque vulnerability groups were defined using PVI scores as follows: 0–1 = least vulnerable, 2–3 = medium, 4–5 = most vulnerable, with 'least vulnerable' (reference group) vs. 'most vulnerable' as main comparison.' Single cell sequencing was performed using 46 plaque segments retrieved from the Athero-Express biobank as described by Slenders *et al.*[22] and[23] (See Supplementary material online, Methods). A total of 20 different cell clusters were identified from 46 patients. We used the addModuleScore (…, assay='RNA',…) within Seurat[24] to calculate module scores for the expression of the selected genes of interest. This module score calculates the average expression levels of the genes differentially on a single plaques cell level, subtracted by the aggregated expression of control gene sets. All analysed genes are binned based on averaged expression, and the control genes are randomly selected from each bin.

2.7 Validation cohort

In Supplementary material online, *Figure S2*, the patient characteristics of the Vienna CEA validation cohort are summarized. 120 patients with carotid artery stenosis undergoing CEA were included in the validation cohort from Medical University of Vienna, Austria. Proteins were extracted using sequential incubation with 0.5 M sodium chloride (NaCl), 0.1% sodium dodecyl sulfate, and 4 M guanidine hydrochloride (GuHCl). All extracts were labelled using tandem mass tags and analyzed on an Orbitrap Fusion Lumos Tribrid MS for proteomics (Thermo Scientific). A parallel reaction monitoring method was developed on a Q Exactive HF MS (Thermo Scientific). ELISA measurements were conducted in plasma samples of the discovery cohort using DuoSet ELISA Ancillary Reagent Kit 2 (DY008B). All clinical investigations were conducted according to Declaration of Helsinki principles. All participants gave written informed consent prior to inclusion in the study. The study of the CEA samples was approved by the local Research Ethics Committee (London, United Kingdom, Research Ethics Committee, REC reference number 08/H0706/129). Summary data and additional analyses that support the findings of this study are available from the corresponding authors on reasonable request. Proteomics and spatial transcriptomics data were deposited at the Proteomics Identifications and Gene Expression Omnibus repositories, respectively.

2.8 Data analysis

Athero-Express CEA samples were divided for subsequent analysis, with subsets used to generate transcriptomic data ($n = 654$), proteomic data ($n = 200$), and single cell sequencing data ($n = 46$). All data were analysed using Rstudio version 2023.06.1 + 524 [Team, R. S. (2020)]. Data are presented as the median ± IQR unless indicated otherwise. Pathway enrichment analysis was performed using the Enrichr[25] or clusterProfiler[26] package. Significant associations between variables were calculated using a linear model with a false discovery rate P-value of <0.05 or adjusted P value (FDR) of <0.05 with BH adjustment. Mean differences between groups were analysed using a t-test or one way ANOVA, with $P < 0.05$ used to determine statistical significance. Correlation analysis was performed using Pearson correlation coefficient test. For the validation cohort, differential expression between clinical and histological characteristics was assessed using DESeq2 R studio package, with $P <$ 0.05 used to determine statistical significance.

3. Results

3.1 Discovery and validation patient cohort

In this study, we used carotid plaques of 200 patients from the Athero-Express biobank study for ECM-proteome analysis (*Figure 1A*). Patients' pre-operative baseline characteristics stratified by PVI scores by dividing into three groups: low vulnerability (LV) (0–1), medium vulnerability (MV) (2–3), and high vulnerability (HV) (4–5) are summarized in *Table 1*. The patient population consists of 51 females and 149 males with a median age of 70. Furthermore, 23% of the patient population suffers from diabetes, 36% are current smokers, 34% have a history of CAD, and 80% have mild to moderate kidney disease (*Table 1*). Notable significant differences include a larger percentage of males and self-reported alcohol use in plaques with higher PVI ($P < 0.05$). In addition, a nominal difference is found in the glomerular filtration rate. The remaining baseline characteristics were not significantly different between the groups. Like the Athero-Express patient population, roughly a quarter of the Vienna validation cohort consisted of female patients with significantly higher HDL levels compared with male patients. Furthermore, Diabetes mellitus type 2 and smoking is more prevalent in male patients compared with female ones. Like the Athero-Express patient population, the Vienna validation cohort does not show a significant difference in the prevalence of major cardiovascular events ($P = 0.4$) (See Supplementary material online, *Table S2* validation cohort Vienna).

3.2 Untargeted proteomics detected a broad spectrum of proteins in atherosclerotic plaques

Atherosclerotic plaque samples ($n = 200$) were enriched for extracellular matrix proteins (to deplete abundant soluble protein histones and ribosomal proteins), digested, and analysed using untargeted proteomics. A total of 2148 proteins were detected, with a mean of 1698 measured proteins per patient (*Figure 1B*). Among the detected proteins, further data processing using Matrisome DB (http://matrisomeproject.mit.edu/) identified 497 ECM and ECM-related proteins, of which 130 were recognized as core ECM proteins. Subsequent data normalisation and quality filtering (the exclusion of proteins based on 30% missing values) resulted in 1499 reliably measured proteins (*Figure 1C*); this set was used for all downstream analyses. Pathway enrichment indicated that these 1499 proteins were involved in multiple biological processes such as the immune response, haemostasis, ECM organisation, transcription/translation, and transport. They were linked to the endoplasmic reticulum, collagen-containing extracellular matrix, and cytosolic ribosome (*Figure 2A*). Individual histological plaque measures as part of the PVI revealed multiple metabolism-related processes involved in plaque macrophage content and fat content, including glycolysis, pyruvate metabolism, and the carbohydrate catabolic process (*Figure 2B*).

3.3 ECM-associated proteins show associations with PVI scores and clinical symptoms

In order to identify the proteins that might underpin the mechanisms involved in plaque destabilisation, we performed a linear regression analysis using protein expression as an outcome and the PVI scores as predictor variable. Plaque stability is assessed using PVI scores, which is defined as

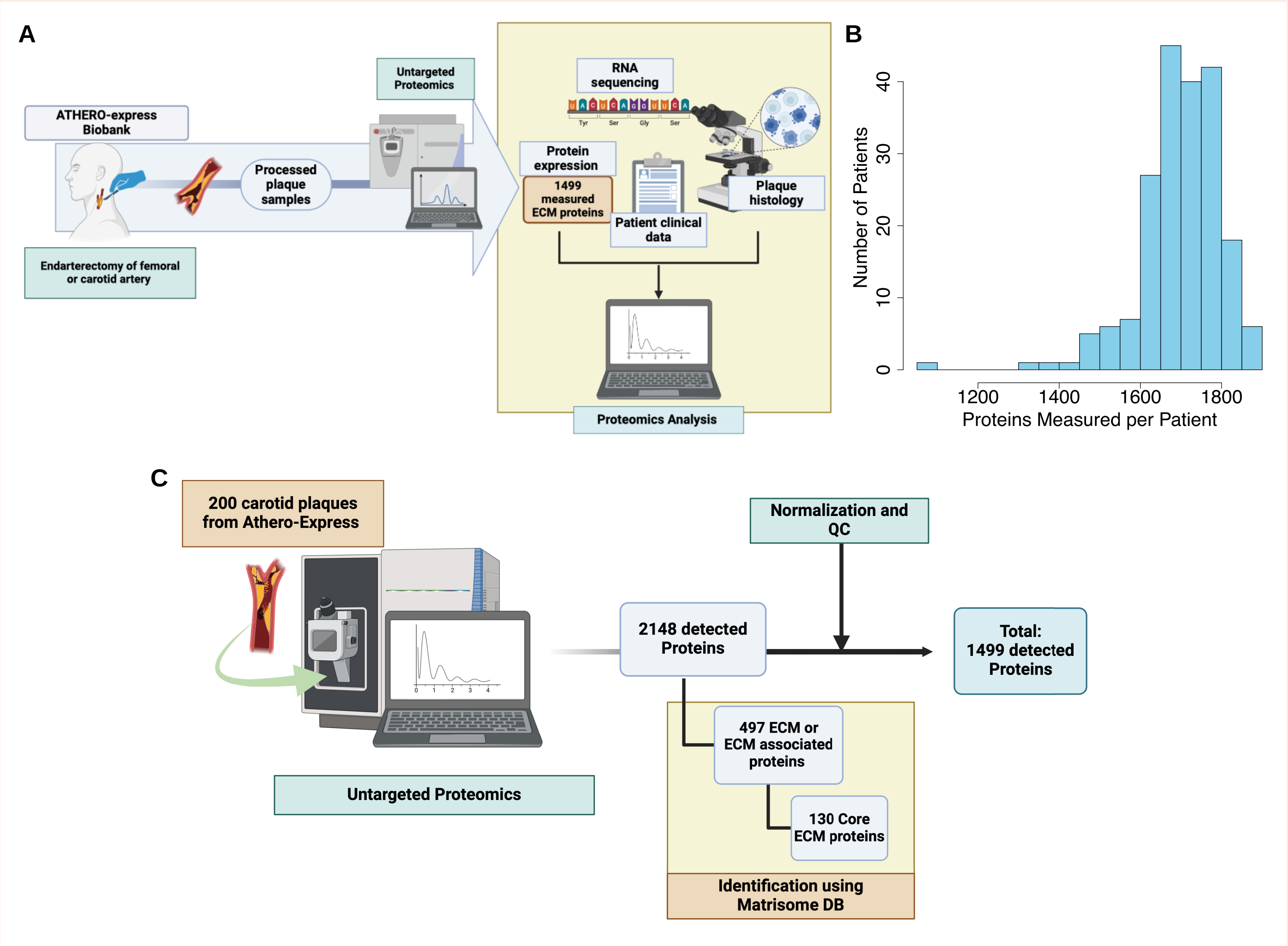

Figure 1 (*A*) A diagram summarising the workflow of this study which included 200 human atherosclerotic plaques. (*B*) Histogram represents the number of measured proteins per patient before quality filtering (mean = 1698). (*C*) Workflow for protein annotation and quality filtering.

Table 1 Summary of patient ($n = 200$) baseline characteristics stratified by PVI

Patient characteristics of all athero-express patients with available proteomic data				
	Plaque vulnerability index score			
	Low vulnerability 0–1	**Medium vulnerability 2–3**	**High vulnerability 4–5**	***P* value**
$N = 200$	**47**	**120**	**33**	
Sex = male (%)	30 (63.8)	89 (74.2)	30 (90.9)	**0.024**
Age yrs [median (IQR)]	71.00 [62.00, 75.00]	70.00 [62.00, 75.00]	71.00 [62.00, 77.00]	0.839
Diabetes status = Yes (%)	12 (25.5)	29 (24.2)	5 (15.2)	0.494
Smoker status (%)				0.373
Never smoked	6 (13.3)	13 (11.3)	8 (24.2)	
Ex-smoker	20 (44.4)	60 (52.2)	14 (42.4)	
Current smoker	19 (42.2)	42 (36.5)	11 (33.3)	
Kidney disease outcomes quality initiative (%)				0.326
Normal kidney function	3 (6.5)	25 (21.0)	7 (21.2)	
Mild chronic kindey disease	27 (58.7)	62 (52.1)	20 (60.6)	
Moderate chronic kidney disease	15 (32.6)	30 (25.2)	6 (18.2)	
Severe chronic kidney disease	1 (2.2)	2 (1.7)	0 (0.0)	
Alcohol use = Yes (%)	29 (65.9)	71 (62.3)	28 (87.5)	**0.026**
Statines = Statines taken (%)	40 (85.1)	88 (73.9)	25 (75.8)	0.303
LDL mmol/L [mean (SD)]	2.63 (0.89)	2.55 (0.92)	3.16 (1.15)	0.335
HDL mmol/L[median (IQR)]	1.06 [0.83, 1.31]	1.06 [0.86, 1.40]	1.01 [0.83, 1.23]	0.655
Total cholesterol mmol/L [mean (SD)]	4.41 (1.04)	4.45 (1.12)	4.96 (1.28)	0.122
Triglycerides mmol/L [median (IQR)]	1.41 [0.96, 1.69]	1.17 [0.98, 1.70]	1.40 [1.06, 1.94]	0.335
Diastoli mmHg [median (IQR)]	80.00 [68.50, 90.00]	80.00 [75.00, 90.00]	82.00 [80.00, 93.00]	0.113
Systolic mmHg [median (IQR)]	155.00 [140.00, 173.00]	151.00 [138.00, 169.00]	160.00 [135.00, 170.00]	0.788
Glomular filtration rate mL/min [mean (SD)]	66.02 (17.53)	73.38 (19.74)	75.89 (18.93)	**0.041**
BMI kg/m^2 [median (IQR)]	26.70 [24.74, 30.79]	26.13 [24.53, 28.54]	26.43 [24.30, 28.63]	0.238
Plasma hsCRP mg/L [median (IQR)]	1.61 [0.89, 4.70]	1.79 [0.73, 4.34]	2.34 [1.16, 8.77]	0.701
CAD history = No CAD history (%)	33 (70.2)	79 (65.8)	20 (60.6)	0.670
Major cardiovcular events = No major events (%)	30 (63.8)	93 (77.5)	26 (78.8)	0.157
Overall plaque phenotype (%)				**<0.001**
Atheromatous	2 (4.3)	36 (30.0)	24 (72.7)	
Fibro-atheromatous	8 (17.0)	55 (45.8)	9 (27.3)	
Fibrous	37 (78.7)	29 (24.2)	0 (0.0)	

Data are presented as percentages/counts or, mean values with standard deviation (SD), or as median values with Interquartile range (IQR). Signficant associations are highlighted in bold.

a semi-quantitative score that summarizes established determinants of plaque destabilisation such as fat content and the presence of macrophage and SMCs[14] (*Figure 3A*). Subsequent linear regression analysis identified 240 proteins that were significantly associated with PVI scores after adjustment for multiple testing, of which S100A8/9, HNRNPA1, and PLIN2 were found among the top 15 most upregulated proteins (*Figure 3B*) (See Supplementary material online, excel *Table S1* for complete results). Subsequent pathway enrichment analysis of 195 positively associated PVI proteins identified more specific connections with biological processes such as immune response, inflammation, and glycolysis (*Figure 3C*). The downregulated 45 PVI proteins exhibited significant associations with biological processes such as ossification and extracellular matrix organisation (*Figure 3C*). Significant differences between PVI levels of vulnerability were found for self-reported alcohol-use and sex in this cohort (*Table 1*). However, when correcting for such confounders, almost all associations between protein expression and PVI remained significant (See Supplementary material online, excel *Table S5*).

PVI scores consist of multiple independent morphological features. In order to determine which histological features could explain the associations found, we performed a correlation analysis between the abundance levels of the 240 PVI-associated proteins and the histological characteristics of the plaques (*Figure 4A*). Strongly correlated trends were observed especially for macrophage content ($R = 0.95$, $P < 0.001$), fat content >10% ($R = 0.95$, $P < 0.001$), and fat content >40% ($R = 0.96$, $P < 0.001$), as well as for overall plaque phenotype ($R = 0.83$, $P < 0.001$), neutrophil content ($R = 0.89$, $P < 0.001$), and plaque haemorrhage ($R = 0.88$, $P < 0.001$) (*Figure 4A*). Our data show that PVI proteins such as HK3, HNRNPA1, and S100A8/9 are among the most positively associated with high macrophage content and fat content. Similarly, our findings indicate that S100A8/9, LTF, and KPNB1 are highly expressed in plaques with plaque haemorrhage, while HK3, S100A8/9, and HNRNPA1 are highly upregulated in plaques with increasing neutrophil content (See Supplementary material online, excel *Table S6*).

3.4 Protein expression levels are not reflected in the transcriptome

To study whether the differences in processes observed between the vulnerability groups were also reflected by differences in transcriptional states in the plaques, we used bulk RNAseq from continuous plaque segments to those used for protein analysis and investigated gene expression

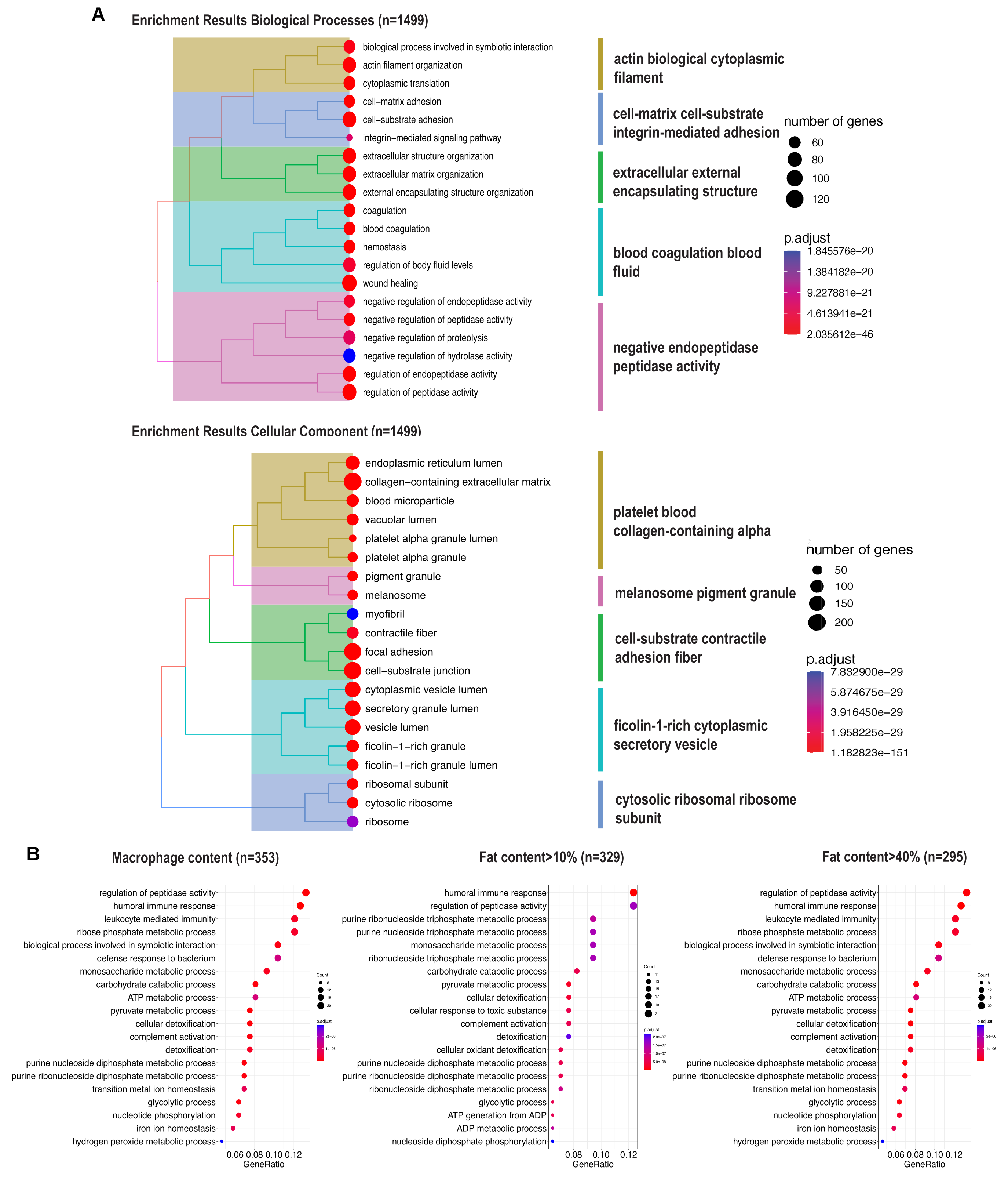

Figure 2 (*A*) Biological processes and cellular components enrichment results for 1499 reliably measured proteins from 200 human atherosclerotic lesions from the Athero-Express biobank. (*B*) Top 20 biological processes enrichment results for proteins significantly associated with macrophage content ($n = 353$, FDR < 0.05) and fat content ($n = 329$; $n = 295$, FDR < 0.05).

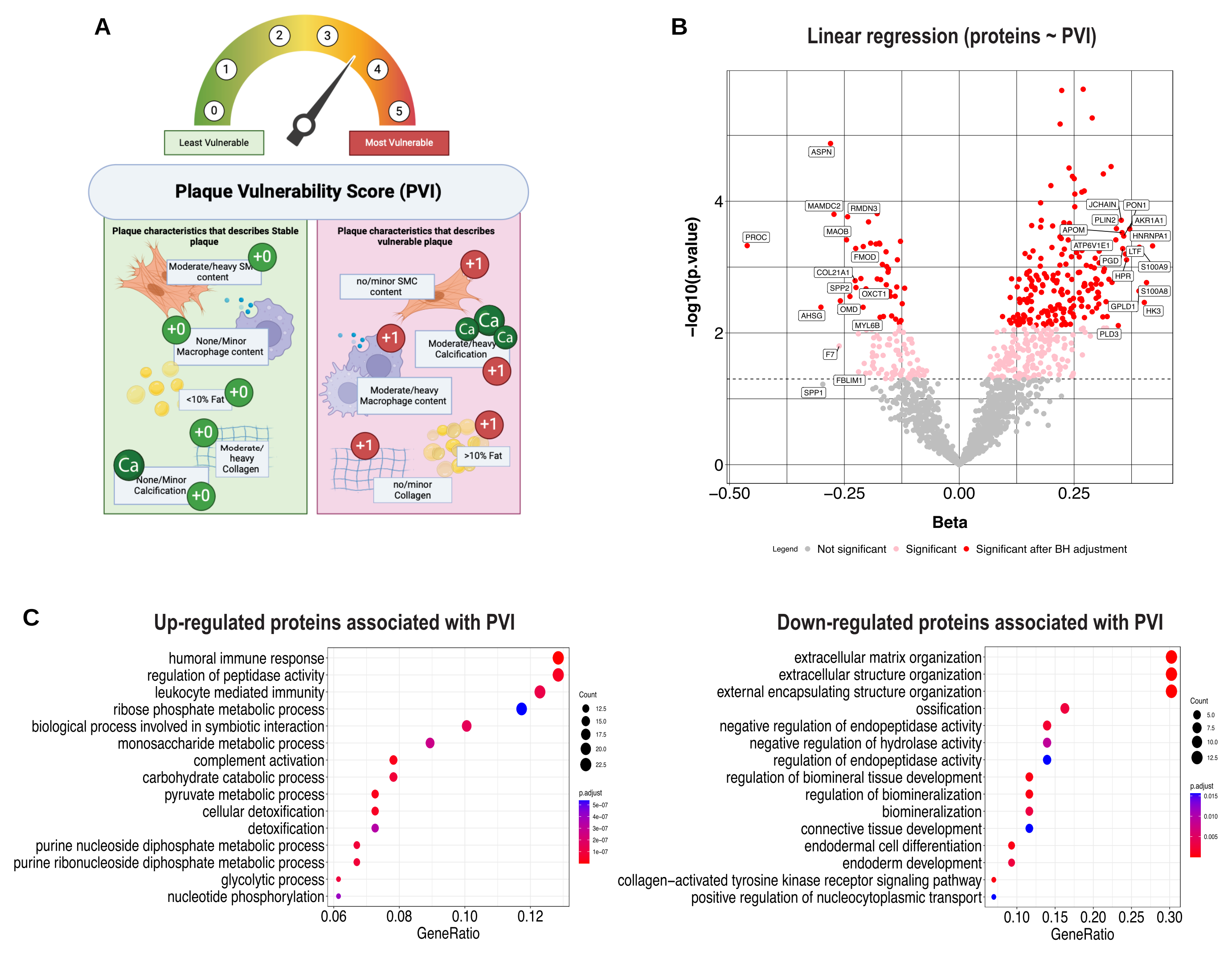

Figure 3 (*A*) Diagram describing PVI score, calculated based on the presence of plaque destabilising and plaque stabilising histological characteristics. (*B*) Volcano plot with top 15 most upregulated and downregulated proteins associated with PVI scores (labelled). The *x*-axis represents the change in protein expression (beta change), and the *y*-axis represents the -log10 *P*-value. Differential protein expression was assessed using a linear regression model, which revealed 240 differentially expressed proteins after BH adjustment (red). Proteins above the dashed gray line are considered nominally significant (pink), with *P*-values <0.05. *n*=200 (*C*) Pathway enrichment results of 240 proteins significantly associated with PVI scores ($P < 0.05$). Left, pathway enrichment results for 195 upregulated differentially expressed proteins. Right, pathway enrichment results for 45 downregulated differentially expressed proteins.

differences between the vulnerability groups (See Supplementary material online, excel *Table S4*). Notably, differential gene expression analysis using transcriptome datasets generated from the same plaque tissue revealed a significant, but weak, correlation with 227 corresponding protein expression differences ($R^2 = 0.19$, $P < 0.001$) (*Figure 4B*). Similarly, many individual proteins, including those with the most significant associations with PVI, showed no or even negative correlation with transcript levels. Among these are genes associated with glycolysis such as HK3, PKM, LDHA, and LDHB (*Figure 4C*).

3.5 Abundance of glycolytic rate-limiting enzymes are associated with plaque vulnerability

Altered metabolism is commonly observed in the progression of various diseases such as cancer, and neurodegenerative disease.[27,28] Similarly, altered glycolytic flux reportedly accelerates disease progression of atherosclerosis in mice.[29] Among the 240 proteins significantly associated with PVI we identified 17 proteins involved in the glycolysis process, of which the glycolysis rate-limiting enzyme HK3 exhibited a positive association with PVI scores ($\beta = 0.40$, $P = 0.003$, $FDR = 0.03$) (See Supplementary material online, excel *Table S1* for complete results). For this reason, we studied the association between glycolysis rate-limiting enzymes with multiple plaque histological characteristics and PVI scores. The rate-limiting enzymes consist of three proteins, namely, Hexokinase (HK), PhosphoFructoKinase (PFK), and Pyruvate Kinase (PK).[30] Another glycolysis enzyme of interest is lactate dehydrogenase (LDH), which is responsible for the conversion of pyruvate into lactate at the end of the glycolysis process. Notably, it has been implicated in the pathogenesis of accelerated atherosclerosis in patients that suffer from diabetes mellitus.[31] The LDHA isoform is predominantly expressed in skeletal muscle and converts pyruvate to lactate, while the LDHB isoform, mainly found in the heart and brain, preferentially converts lactate to pyruvate (LDHB).[32]

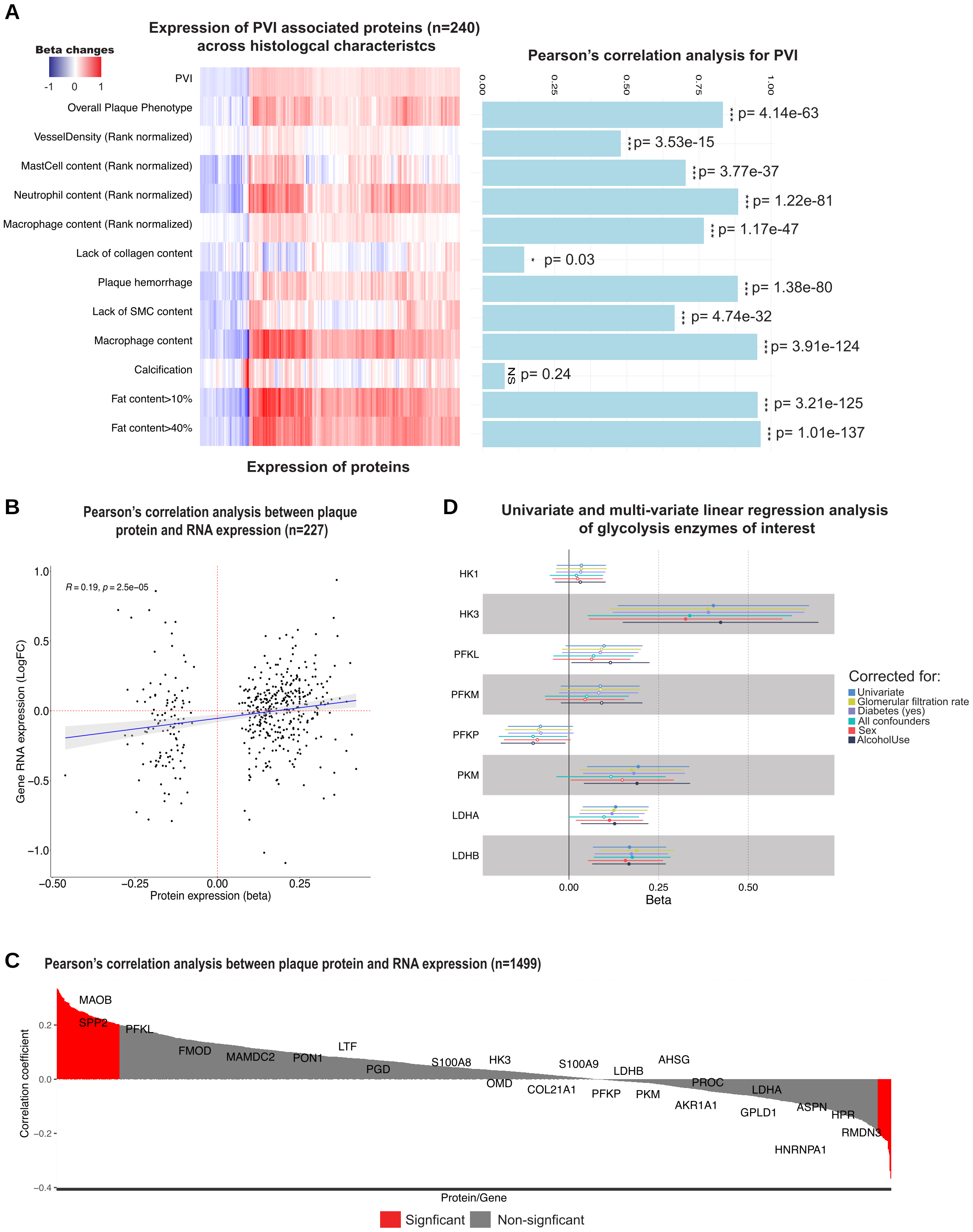

Figure 4 (*A*) Left, heatmap depicting the difference in expression of the 240 proteins associated with PVI across multiple plaque characteristics generated from 200 human CEA plaques. Right, bar plot with a corresponding correlation coefficient between PVI and multiple plaque characteristics. (*B*) Correlation plot between RNA expression and protein expression changes of 227 proteins significantly associated with PVI scores. (*C*) Correlation between RNA and protein ($n = 1499$) expression, with significantly correlated proteins highlighted in red and non-significant correlation highlighted in gray. Proteins of interest are labelled. The correlation coefficients in (*A*, *B*, and *C*) were calculated using Pearson's correlation, with $P < 0.05$ considered statistically significant. (*D*) Univariate and multi-variate analysis for six glycolysis rate-limiting enzymes. Beta changes were calculated by performing a linear regression model. In blue, are results for univariate regression between glycolytic enzymes and PVI. In dark yellow, multi-variate regression results between glycolytic enzymes and PVI corrected for glomerular filtration rate. In purple, multi-variate regression results between glycolytic enzymes and PVI corrected for Diabetes. In turquoise, multi-variate regression results between glycolytic enzymes and PVI with all confounders present together. In red, multi-variate regression results between glycolytic enzymes and PVI corrected for Sex. In black, multi-variate regression results between glycolytic enzymes and PVI corrected for self-reported alcohol-use. Filled in dots indicate significant associations ($P < 0.05$).

The proteomics data contained expression data for the following proteins with those enzymatic activities: HK1, HK3, PFKL, PFKM, PFK, PKM1/2 (PKM), LDHA, and LDHB.

Subsequent linear regression analysis revealed significant differences between the expression levels of glycolysis enzymes and PVI scores, including enzymes HK3, PKM, LDHA, and LDHB ($\beta = 0.40$, $P = 0.003$, FDR = 0.03; $\beta = 0.19$, $P = 0.009$, FDR = 0.05, $\beta = 0.13$, $P = 0.006$, FDR = 0.03; $\beta = 0.17$, $P = 0.001$, FDR = 0.02) ('Univariate', *Figure 4B*).

Significant differences between PVI groups were found for self-reported alcohol-use and sex in this cohort (*Table 1*). Therefore, in order to test whether the association of glycolytic proteins with PVI was confounded by these, we performed a multi-variate linear regression to assess the effects of these confounders. Although no significant differences were found between diabetic and non-diabetic patients in association with PVI (*Table 1*; $P = 0.494$), we still included patient diabetes status in the multi-variate analysis, given its implication in the pathogenesis of atherosclerosis reported in previous literature.[33] The observed elevated levels of glycolysis enzymes in high PVI plaques were found to be partly confounded by these risk factors. However, HK3, PKM, LDHA, and LDHB, all remained significantly associated with PVI scores after adjusting for these confounders independently (*Figure 4B*). Furthermore, a multi-variate linear regression model revealed that PKM and LDHA, are negatively associated with PVI in diabetic patients ($\beta = -0.44$, $P = 0.038$; $\beta = 0.37$, $P = 0.007$; respectively). A similar negative relationship was found for HK3; however, this was not statistically significant ($\beta = -0.49$, $P = 0.213$). After adjusting for all confounders, including patient diabetic status (Diabetic: yes), only HK3, LDHB, and PFKP remained significantly associated with PVI.

Subsequent histological analysis revealed that HK3, PFKL, PKM, LDHA, and LDHB showed significantly elevated expression in plaque with high levels of macrophage and fat content, which are both indicators of vulnerable plaques (*Figure 5A*). Further analysis revealed a strong positive correlation between LDHA protein expression ($R^2 > 0.7$, $P < 0.001$) and HK3, PFKL, and PKM glycolysis rate-limiting enzymes (*Figure 5B*). As for LDHB, the protein demonstrated a weaker positive yet significant correlation with the HK3, PFKL, and PKM.

3.6 Glycolytic rate-limiting enzymes expression in plaque cells

In order to assess which plaque cells are potentially responsible for this observed increased presence of glycolytic enzymes (HK1, HK3, PFKL, PKM, PFKP, PFKM, LDHA, and LDHB), previously generated single-cell sequencing data, derived from different patients of the same cohort (see Supplementary material online, excel *Table S3*)[22] was analysed. Expression of the equivalent genes for each protein was projected onto the single-cell clusters derived from plaques within the same cohort and the module score was calculated. The selected glycolysis rate-limiting enzymes were expressed in multiple plaque cell types including endothelial cells, SMCs, inflammatory macrophages, and foam cells (*Figure 5C*). In comparison, downregulated proteins associated with PVI, which belonged to pathways such as ossification and extracellular matrix organisation, were more highly expressed in endothelial cells and SMCs (*Figure 5C*). Further analysis revealed that most of the glycolysis enzymes of interest are highly expressed in inflammatory macrophages, foam cells and SMCs, and they exhibit expression in other cell types, such as endothelial cells and dendritic cells. HK3, in comparison, is almost exclusively elevated in inflammatory macrophages and foam cells (*Figure 5D*). Anti-HK3 plaque staining further supports this finding, showing clear overlap between areas with high macrophage content and elevated HK3 expression (*Figure 5E*) (See Supplementary material online, PDF *Figure S1*).

3.7 Glycolysis rate-limiting enzymes are higher expressed in the core and associated with symptoms in a validation cohort

Finally, we validated the significant differences between the glycolysis rate-limiting enzymes using proteomics data from 121 atherosclerotic plaques from CEA patients from a validation cohort (University of Vienna) (See Supplementary material online, PDF *Table S8*). The carotid endarterectomies from the validation cohort were divided into peripheral and core (culprit) specimens as the two artery regions differed in their proteomic profile.[34] Multiple glycolysis enzymes of interest were found significantly upregulated in core atherosclerotic lesions and symptomatic patients (*Figure 6A*). Correspondingly, our data showed significantly elevated presence of glycolytic enzymes in patients presenting with severe symptoms (TIA and stroke) in comparison to those with milder symptoms (asymptomatic and ocular), specifically for HK3, PFKM, PFKL, and LDHA ($\beta = 0.761$, $P = 0.031$; $\beta = 0.388$, $P = 0.006$; $\beta = 0.329$, $P = 0.014$; $\beta = 0.234$, $P = 0.039$, respectively) (*Figure 6B*).

3.8 Glycolytic enzymes are strongly associated with BLVRB expression

PVI-associated proteins show similar associations to plaque haemorrhage ($R = 0.88$, $P < 0.001$) (*Figure 4A*). Among these are proteins with a significant relationship with plaque haemorrhage such as S100A8, S100A9, LTF, and BGN ($\beta = 0.58$, $P = -0.03$; $\beta = 0.65$, $P = 0.04$; $\beta = 0.58$, $P = 0.03$; $\beta = -0.29$, $P = 0.01$, respectively). Another protein among these is Biliverdin IXβ reductase (BLVRB), which is a key enzyme in Hb metabolism that has been identified as a valuable plasma biomarker for IPH and clinical symptoms.[35] This enzyme, downstream of HMOX1, is responsible for the final conversion of biliverdin to bilirubin and iron (Fe 2+).[36] In concordance with previous studies, we observed a significantly elevated expression of BLVRB in in symptomatic patients of the Athero-Express cohort ($P = 0.027$) (*Figure 6C*). Furthermore, a significant positive association between BLVRB expression and higher levels of PVI scores was found ($\beta = 0.26$, $P = 0.001$), indicating that plaque BLVRB protein expression is associated with vulnerable plaques (*Figure 6C*). Notably, the expression of BLVRB is highly associated with CD68+ cells, such as macrophages.[36] This was confirmed in the Athero-Express cohort in which inflammatory cells such as resident macrophages, inflammatory macrophages, and foam cells, were found predominantly responsible for the expression of BLVRB (*Figure 6D*). Given the observed increased abundance of glycolysis enzymes in inflammatory cells and in more vulnerable plaques, we investigated how BLVRB expression is associated with the expression of glycolytic enzymes. After analysis, a significant positive association was found between BLVRB expression and glycolysis rate -limiting enzymes HK1, PFKL, PFKM, PKM, and HK3 especially (all, $P < 0.001$, FDR < 0.001) (*Figure 6E*). Downstream glycolysis enzymes, LDHA and LDHB, were also significantly elevated with higher levels of BLVRB ($b = 0.27$, $P < 0.001$, FDR < 0.001; $b = 0.30$, $P < 0.001$, FDR < 0.001) (*Figure 6E*).

3.9 The difference in glycolysis rate-limiting enzymes between HV and LV lesions is larger in women than in men

Previous literature has provided evidence that atherosclerosis plaque progression diverges between the sexes at the histological and transcriptomic levels.[23,37] Therefore, crucial differences may exist between key processes that determine the pathogenesis of atherosclerosis, such as inflammation and the immune response.[38] Given the observed association between the glycolysis enzymes and plaque macrophage content within our cohort, we wanted to assess if there are major expression differences between female and male plaque lesions.

Female ($n = 51$) and male ($n = 149$) patients in our cohort show significant differences in HDL cholesterol levels (1.29 mmol/L vs. 1.08 mmol/L, $P = 0.006$), frequency of major adverse cardiovascular events within 3 years (29.5% vs. 13.7%, $P = 0.04$), and overall plaque phenotype (*Table 2*). The difference in HDL concentration is to be expected as women are known to possess higher HDL concentrations compared with men.[39,40] All other baseline characteristics remained similar between the two sexes.

Linear regression analysis demonstrated significantly elevated expression of HK3, PKM, PFKL, PFKM, and LDHA in male atherosclerotic lesions

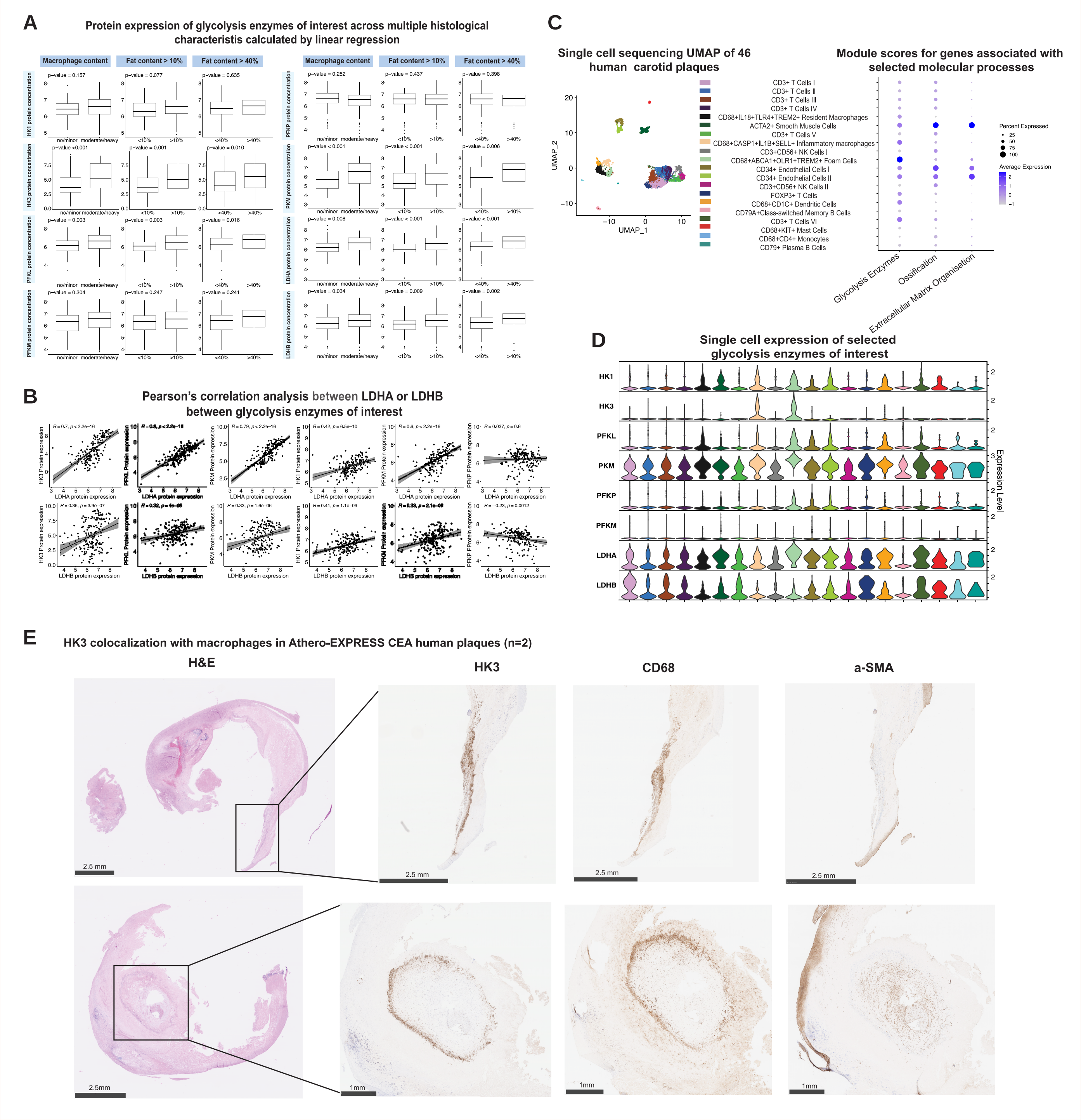

Figure 5 (*A*) Expression of eight glycolysis enzymes of interest across multiple histological characteristics from 200 atherosclerotic lesions from the Athero-Express biobank. The associations between the glycolysis enzymes and multiple histological characteristics were calculated using a linear regression model, with $P < 0.05$ considered significant. (*B*) Correlation plots between LDHA/B protein expression and six glycolysis rate-limiting enzymes. Correlation coefficients were calculated using Pearson's correlation, with $P < 0.05$ considered statistically significant. (*C*) Left, UMAP showing single cell sequencing data from 46 human carotid atherosclerotic plaques. Right, module scores calculated with genes associated with selected molecular processes. (*D*) Single cell expression (*n* samples =46) of six selected glycolysis enzymes. (*E*) (H & E) stainings of CEA plaques ($n = 2$) with moderate/heavy macrophage content and corresponding HK3, CD68, and α-SMA staining's.

compared with female lesions (*Figure* 7*A*). Subsequent sex-stratified linear regression analysis showed a stronger association of PVI scores with glycolytic enzymes in females compared with males. Five of the eight glycolytic enzymes significantly associated with PVI in female-only dataset, whereas in the male-only dataset, only two glycolytic enzymes show significant association with PVI (*Figure* 7*B and C*). Furthermore, a significant interaction

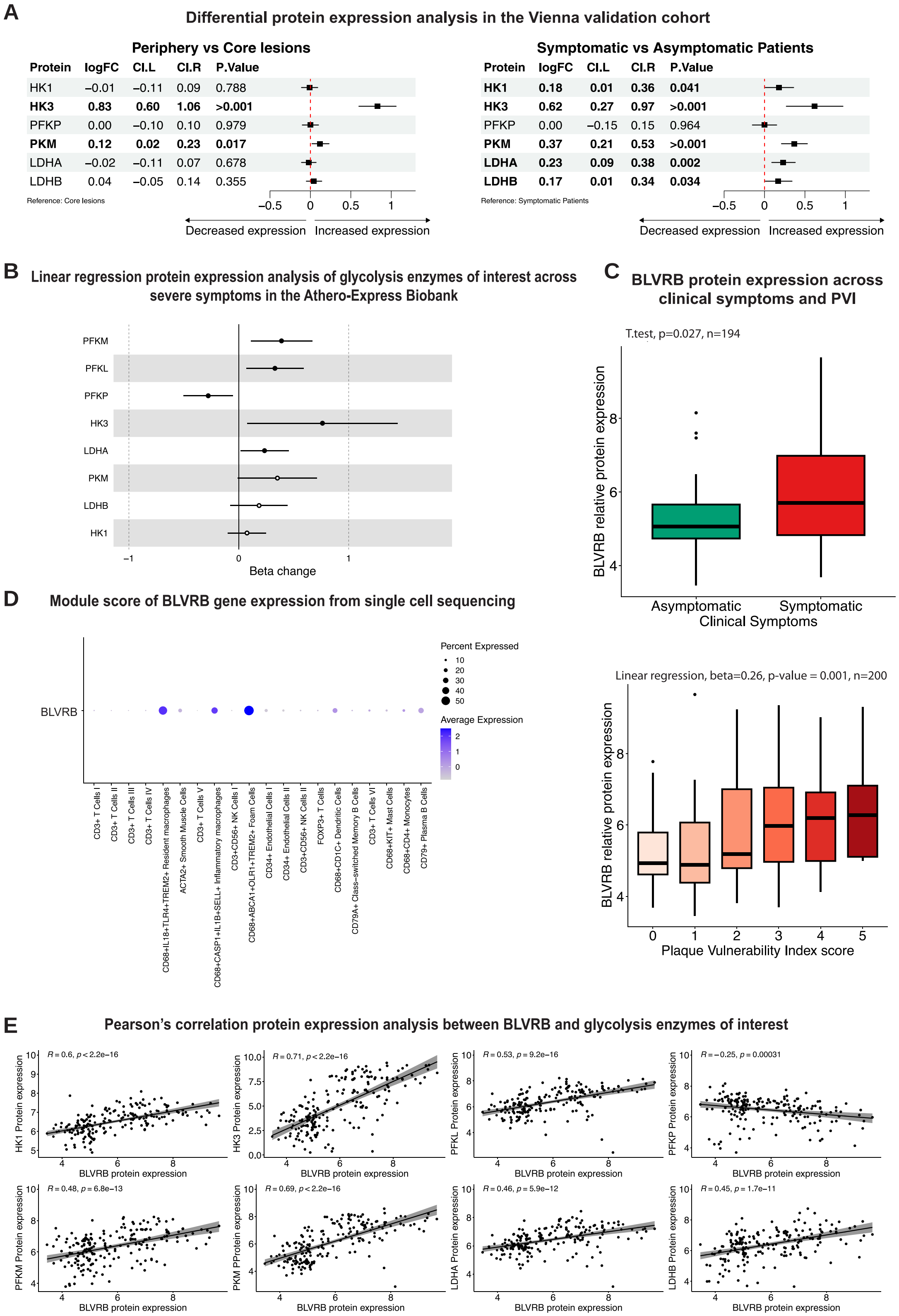

A Differential protein expression analysis in the Vienna validation cohort

Periphery vs Core lesions

Protein	logFC	CI.L	CI.R	P.Value
HK1	–0.01	–0.11	0.09	0.788
HK3	**0.83**	**0.60**	**1.06**	**>0.001**
PFKP	0.00	–0.10	0.10	0.979
PKM	**0.12**	**0.02**	**0.23**	**0.017**
LDHA	–0.02	–0.11	0.07	0.678
LDHB	0.04	–0.05	0.14	0.355

Reference: Core lesions

Symptomatic vs Asymptomatic Patients

Protein	logFC	CI.L	CI.R	P.Value
HK1	**0.18**	**0.01**	**0.36**	**0.041**
HK3	**0.62**	**0.27**	**0.97**	**>0.001**
PFKP	0.00	–0.15	0.15	0.964
PKM	**0.37**	**0.21**	**0.53**	**>0.001**
LDHA	**0.23**	**0.09**	**0.38**	**0.002**
LDHB	**0.17**	**0.01**	**0.34**	**0.034**

Reference: Symptomatic Patients

B Linear regression protein expression analysis of glycolysis enzymes of interest across severe symptoms in the Athero-Express Biobank

C BLVRB protein expression across clinical symptoms and PVI

D Module score of BLVRB gene expression from single cell sequencing

E Pearson's correlation protein expression analysis between BLVRB and glycolysis enzymes of interest

Figure 6 (*A*) Forest plot with associations between six glycolysis associated enzymes and histological (left) or clinical traits (right) in the CEA Vienna cohort ($n = 120$). Protein expression is expressed in log fold changes on the *x*-axis with lower and upper confidence intervals. Significant expression differences were assessed using differential expression analysis DESeq2 R package. Significant protein associations are highlighted in bold ($P < 0.05$). (*B*) Forest plot showing the relationship between six glycolysis associated enzymes and severe clinical symptoms (TIA + Stroke) from 200 Athero-Express plaque samples. Each protein is represented on the *y*-axis, while protein expression is expressed in beta changes and standard deviation on the *x*-axis. Significant protein associations are (continued)

Figure 6 Continued
highlighted with black dot ($P < 0.05$). Beta changes and P values were calculated using linear regression model. (*C*) Expression of BLVRB enzyme (*y*-axis) across clinical symptoms or PVI score (*x*-axis). Mean protein expression differences between BLVRB expression and clinical symptoms in 194 patients were assessed using a *t*-test, with $P < 0.05$ considered statistically significant. Protein expression differences between BLVRB and PVI score were assessed in 200 plaque lesions by performing a linear regression model, with $P < 0.05$ considered statistically significant. (*D*) Single cell expression of BLVRB from 46 Athero-Express samples. (*E*) Scatterplots showing the correlation between eight glycolysis associated enzymes and BLVRB protein expression. Pearson's correlation coefficients were calculated using Pearson's correlation, with $P < 0.05$ considered statistically significant.

effect of sex is identified on the association between PVI and most of the glycolytic enzymes, except for HK1, PFKP, and LDHB (*Table 3*).

Previous literature has attributed elevated levels of glycolysis enzymes due to the high presence of macrophages, which undergo metabolic reprogramming in more vulnerable plaques.[41] This phenomenon is particularly notable in male atherosclerotic lesions, which are characterized by high presence of macrophages. Female lesions, in contrast, are commonly described with low levels of macrophages and high SMC content. Therefore, sex-stratified histological analysis was performed to uncover any sex-specific differences. As a result, significantly increased expression of glycolysis enzymes HK3, LDHA, PFKM, and PKM ($\beta = 1.55$, $P = 0.02$ and $\beta = 1.82$, $P = 0.017$; $\beta = 0.52$, $P = 0.02$ and $\beta = 0.58$, $P = 0.02$; $\beta = 0.63$, $P = 0.01$ and $\beta = 0.64$, $P = 0.03$; $\beta = 0.98$, $P = 0.003$ and $\beta = 0.82$, $P = 0.04$, respectively) was found in vulnerable female-only plaques with both moderate/heavy macrophage content as expected; however, an increased level of these proteins was associated with no/minor SMC content (*Figure 7E*). Although the male-only dataset also exhibits similar associations between the glycolytic enzymes and macrophage content as compared with the female-only dataset, an inverse trend is observed, in which male plaques with no/minor SMC content exhibit decreased expression of glycolytic enzymes.

4. Discussion

In this study we have employed proteomic analyses in 200 male and female human atherosclerotic plaques to identify the molecular mechanisms associated with vulnerable plaques. With the help of untargeted proteomics analysis, we have identified 1499 plaque proteins, which are involved in multiple biological processes such as the immune response, haemostasis, ECM organisation, transcription/translation, and transport. Subsequent linear regression analysis identified 240 plaque proteins significantly associated with PVI scores. Biological processes such as inflammation, and glycolysis were among the top enrichment terms within these proteins. Notably, HK3, a glycolysis rate-limiting enzyme, was found among the top 10 most upregulated proteins associated with PVI. Given these findings, our focus was drawn towards further investigating the role of glycolysis in atherosclerosis plaque stability using multi-omics approaches and histology. Although power was limited, our data suggest that glycolysis enzymes have a stronger relation with PVI in women compared with men.

4.1 The plaque transcriptome and proteome are weakly correlated

Previous studies have attempted to define the molecular profile of atherosclerosis by relying on transcriptomic data.[42] However, our results suggest that the transcriptome alone cannot thoroughly describe the underlying mechanisms of atherosclerosis. This assertion is substantiated by the identification of a weak correlation between the transcriptome and the proteome expressed within the plaque. Among the 1499 proteins that we detected in the plaque, only 8% were found significantly correlated with RNA expression. This is partly explained by the shorter half-life experienced by RNA molecules compared with protein.[43,44] Another explanation is found in proteins which RNA expressions do not originally occur within the plaque. For example, PROC, AHSG, and CTSG, which are among the topmost upregulated proteins within the plaque, did not correlate significantly with plaque RNA expression because these genes are preferentially expressed in the liver or bone-marrow and lymphoid tissues. Furthermore, due to the significantly shorter half-life of RNA molecules, transcriptomic data helps delineate the acute processes involved in atherosclerosis plaque progression, while protein expression reflects the more long-term processes that contribute to plaque development, which may involve proteins from external sources.

Given these differences, potential molecular pathways of interest may become overlooked when relying on transcriptomic data alone. Therefore, both transcriptomic and proteomic data should be analysed in tandem to help shed light on the mechanisms of atherosclerosis. This underlines the importance of multi-omic approaches as one omics data layer does not necessarily reflect all processes present in the tissue.

Previously, we and others have identified individual proteins that were studied in relation to plaque composition in the Athero-Express biobank, such as Forkhead box protein P1 (FOXP1), whose expression was immunohistochemically observed in multiple cell types in human atherosclerotic plaque lesions. FOXP1 was associated with stable plaque characteristics and increased collagen and EGR1 expression.[45] Another example is the identification of adipocyte fatty acid binding protein, which was significantly associated with a two-fold increase in the risk for vascular events or vascular intervention during follow-up in immunohistochemical stainings of human atherosclerotic plaques.[46]

4.2 Elevated glycolytic enzyme expression is associated with plaque destabilisation in human atherosclerotic lesions

The role of the Immune response and inflammation in the disease progression of atherosclerosis has long been established by others.[47–49] Therefore, the observed significant association between the PVI associated proteins with immune response and inflammation was expected. However, the significant association between measures of PVI and the glycolytic process has not been clearly demonstrated in human atherosclerotic tissue. Previous studies, largely in mice, have confirmed that metabolic reprogramming, such as changes in glycolysis, can take place in atherosclerotic disease and are involved in endothelial dysfunction, inflammation, vascular smooth muscle cell (VSMC) proliferation, and thrombosis.[29,50,51] Therefore, key proteins associated with the regulation of the glycolysis process may contribute to atherosclerosis plaque progression. For this reason, we studied the association between glycolysis rate-limiting enzymes with multiple plaque characteristics and PVI scores. Through proteomic analysis, we have identified a significant association with PVI and three glycolysis rate-limiting enzymes (HK, PFK, PK), which hinted at elevated glycolytic activity in vulnerable plaques. Further histological analyses provided additional support, demonstrating a strong positive association between increasing glycolysis rate-limiting enzyme expression in plaques with heavy/moderate macrophage content and fat content, both contributors to plaque vulnerability. The strong association between plaque vulnerability and glycolysis can be explained by the influence of glycolysis in various cell types, with functions that critically determine disease progression of atherosclerosis.[52] For example, the metabolic transition to glycolysis is known to be crucial for pro-inflammatory M1 macrophage proliferation, suggesting that the heightened levels of glycolysis rate-limiting enzymes indicate the presence of pro-inflammatory activation of macrophages within the plaque.[53] The

Table 2 Summary of patient baseline characteristics ($n = 200$) stratified by sex

	Overall	**Female**	**Male**	***P* value**
N	200	51	149	
Age yrs [median (IQR)]	70.00 [62.00, 76.00]	70.00 [62.00, 74.50]	71.00 [62.00, 76.00]	0.322
Diabetes status = Yes (%)	46 (23.0)	8 (15.7)	38 (25.5)	0.213
Smoker status (%)				0.146
Never smoked	27 (14.0)	9 (18.4)	18 (12.5)	
Ex-smoker	94 (48.7)	18 (36.7)	76 (52.8)	
Current smoker	72 (37.3)	22 (44.9)	50 (34.7)	
Kidney disease outcomes quality initiative (%)				0.331
Normal kidney function	35 (17.7)	7 (14.0)	28 (18.9)	
Mild chronic kindey disease	109 (55.1)	29 (58.0)	80 (54.1)	
Moderate chronic kidney disease	51 (25.8)	12 (24.0)	39 (26.4)	
Severe chronic kidney disease	3 (1.5)	2 (4.0)	1 (0.7)	
Alcohol use = Yes (%)	128 (67.4)	28 (58.3)	100 (70.4)	0.172
Statines = Statines taken (%)	153 (76.9)	40 (80.0)	113 (75.8)	0.682
LDL mmol/L [mean (SD)]	2.73 (0.96)	2.63 (1.11)	2.76 (0.91)	0.531
HDL mmol/L[median (IQR)]	1.06 [0.84, 1.36]	1.25 [0.96, 1.55]	1.03 [0.83, 1.29]	**0.017**
Total cholesterol mmol/L [mean (SD)]	4.53 (1.14)	4.67 (1.32)	4.49 (1.09)	0.433
Triglycerides mmol/L [median (IQR)]	1.27 [0.98, 1.70]	1.40 [0.99, 1.87]	1.26 [0.98, 1.70]	0.573
Diastoli mmHg [median (IQR)]	80.00 [73.00, 90.00]	80.00 [76.00, 90.00]	80.00 [70.00, 90.00]	0.569
Systolic mmHg [median (IQR)]	153.00 [138.00, 170.00]	160.00 [135.00, 170.00]	150.00 [138.00, 168.00]	0.554
Glomular filtration rate mL/min [mean (SD)]	72.09 (19.34)	68.70 (19.05)	73.23 (19.36)	0.152
BMI kg/m^2 [median (IQR)]	26.27 [24.49, 29.27]	26.56 [24.95, 29.75]	26.23 [24.49, 28.98]	0.500
Plasma hsCRP mg/L [median (IQR)]	1.77 [0.87, 4.65]	2.25 [0.96, 6.35]	1.68 [0.72, 4.30]	0.187
CAD history = No CAD history (%)	132 (66.0)	36 (70.6)	96 (64.4)	0.529
Major cardiovcular events = No major events (%)	149 (74.5)	44 (86.3)	105 (70.5)	**0.040**
Overall plaque phenotype (%)				**0.044**
Atheromatous	62 (31.0)	9 (17.6)	53 (35.6)	
Fibro-atheromatous	72 (36.0)	20 (39.2)	52 (34.9)	
Fibrous	66 (33.0)	22 (43.1)	44 (29.5)	

Data are presented as percentages/counts or, mean values with standard deviation (SD), or as median values with Interquartile range (IQR). Significant associations are highlighted in bold.

resulting heightened pro-inflammatory macrophage activity can contribute to plaque vulnerability and the disruption of the renewal of structural elements that promote mechanical stability.[53] Thus, inhibiting HK3 may have stabilising effects, as previously reported with corosolic acid, a potent HK3 inhibitor, in treated apolipoprotein E-deficient mice.[54,55] Another example of abnormal metabolism in plaque cells is the transition of contractile into synthetic SMCs.[56] During arterial injury, lipid infiltration, and inflammatory stimulation, SMCs switch to a synthetic phenotype which is characterized by a lower level of contractile proteins, higher ECM component expression, and ECM remodelling enzymes. Following the switch, SMCs can exacerbate plaque development by migrating into the intima where they are able to take up ox-LDL and transition into new foam cells.[51,56] SMC phenotype switching is triggered by lactate, which accumulates when LDH converts pyruvate, another product of glycolysis, into lactic acid during enhanced glycolytic activity in atherosclerosis.[57] Furthermore, expression of glycolysis rate-limiting enzymes in single cell RNA sequencing was found in SMC, inflammatory macrophages, and foam cells in atherosclerotic plaques. Additionally, histological analysis revealed significantly elevated levels of rate-limiting glycolysis enzyme proteins in plaques with moderate to high macrophage content.

Thus, high levels of extracellular lactate could be expected in more vulnerable plaques, though further analysis of plaque lysates are required to confirm this hypothesis. Indeed, increased blood lactate concentrations have been observed in a previous cross-sectional study in association with carotid atherosclerosis.[58] Furthermore, lactate has been reported to be enriched in the necrotic core, whereas pyruvate can promote fibrous cap formation and PK M2 has been identified as a key regulator of murine SMC function in vascular remodelling.[59,60]

Our observed heighted expression of glycolytic enzymes, the expression of which was detected in inflammatory macrophages, SMCs, and foam cells in 200 human atherosclerotic lesions further corroborates our hypotheses that elevated presence of glycolytic enzymes may be involved in pro-inflammatory and plaque destabilising effects.

4.3 More vulnerable female atherosclerotic lesions exhibit a more pronounced presence of glycolysis rate-limiting enzymes

Major differences exist between male and female atherosclerotic lesions, such as plaque composition and symptoms. Some well-known reported characteristics are a larger plaque size, more calcification, lipid-rich necrotic core, and a higher risk for intraplaque haemorrhage, which occur more frequently in male cases compared with female ones.[37,61] Previous molecular phenotyping of atherosclerotic plaques by sex has also uncovered gene regulatory networks that point to different networks within fibrous lesions that are common in women.[23,62] In this study, we have uncovered that sex differences extends further into the proteome where glycolysis rate-limiting enzymes are found in significantly elevated levels in more vulnerable male plaques. However, we also identified that the increase in

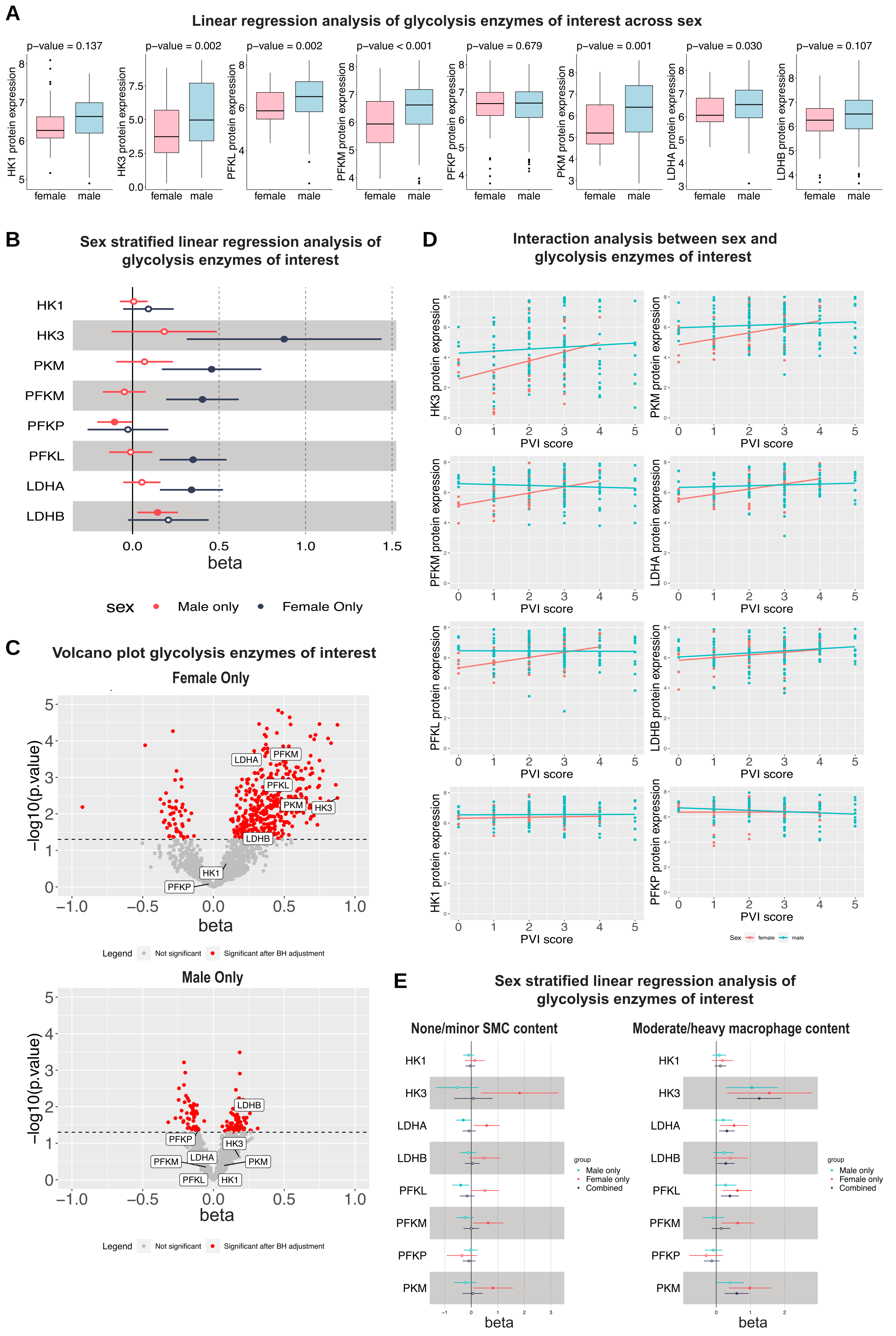

Figure 7 (*A*) The expression of eight selected glycolysis proteins across sex (149 males; 51 females). Protein expression differences in (*A*, *B*, *C*, and *E*) were assessed using a linear regression model, with $P < 0.05$ considered significant. (*B*) Beta changes for eight selected proteins associated with PVI in male-only ($n = 149$) and female-only ($n = 51$) datasets. Significant associations with PVI are highlighted with filled in dot. (*C*) Volcano plots showing differentially expressed

(continued)

Figure 7 Continued
proteins associated with PVI in male-only ($n = 149$) and female-only ($n = 51$) datasets in a volcano plot. The *x*-axis represents the change in protein expression (beta change), and the *y*-axis represents the -log10 *P*-value. Proteins above the dashed gray line are considered significant, with *P*-values <0.05. *D*) Interaction plots for eight selected glycolysis proteins demonstrating relationship between PVI and glycolysis enzyme expression across sex (149 males; 51 females). *E*) Beta changes in the expression of eight glycolysis enzymes are shown between plaques with none/minor SMC and moderate/heavy macrophage content. Significant differences in enzyme expression are indicated by filled in dot.

Table 3 Summary of interaction analysis results for eight glycolysis enzymes with additional sex stratified analysis with female and male only datasets

Interaction effect PVI*Sex

Protein		**beta**	***P* value**	
HK1				
	Male only	0.007	0.869	
	Female only	0.09	0.225	
	Interaction effect (female)	0.08	0.341	
HK3				
	Male only	0.18	0.241	
	Female only	0.88	**0.004**	**
	Interaction effect (female)	0.69	**0.042**	*
PKM				
	Male only	0.06	0.41	
	Female only	0.46	**0.003**	**
	Interaction effect (female)	0.39	**0.033**	*
PFKM				
	Male only	−0.048	0.454	
	Female only	0.404	**<0001**	***
	Interaction effect (female)	0.452	**0.001**	**
PFKL				
	Male only	−0.011	0.865	
	Female only	0.35	**<0001**	***
	Interaction effect (female)	0.361	**0.008**	**
PFKP				
	Male only	−0.1	**0.042**	*
	Female only	−0.027	0.823	
	Interaction effect (female)	0.077	0.512	
LDHA				
	Male only	0.054	0.055	.
	Female only	0.341	**<0001**	***
	Interaction effect (female)	0.287	**0.015**	*
LDHB				
	Male only	0.144	**0.017**	*
	Female only	0.207	0.088	
	Interaction effect (female)	0.06	0.639	

Beta changes and *P*-values were calculated using interaction linear regression model, with $P < 0.05$ considered statistically significant. *$P < 0.05$, **$P < 0.01$, ***$P < 0.001$.

glycolysis enzyme protein expression is more pronounced in female plaques as PVI scores increases. This may indicate that the increased presence of glycolysis enzymes may play a larger role in female atherosclerosis plaque stability. Furthermore, the structural differences between female and male atherosclerotic lesions could warrant an additional explanation for the more profound elevated expression of glycolysis rate limiting enzymes seen in female lesions. For example, female plaques with no/minor SMCs content exhibited higher levels of glycolysis enzyme expression. In fact, previously reported evidence supports that SMC to myofibroblast transition, which was found to be high in female plaques,[23,62] is dependent on aerobic glycolysis and its inhibition would reduce expression of multiple ECM genes, which are essential for lesion-stabilising functions.[63] Therefore, the altered metabolic activity in the plaque may be in part driven by loss of SMC content in addition to macrophage content in female plaques.

Nevertheless, it is important to note the large population bias for male samples. Therefore, additional female samples are required to confirm these findings.

4.4 High glycolysis activity may be a sign of IPH

Enhanced glycolysis in pro-inflammation macrophages has been reported to drive reactive oxygen species-mediated Il-1b production and tumour necrosis factor translation.[29] However, this association has been thoroughly described previously. A potential alternative connection lies in the expression of BLVRB and its implication in IPH and adverse cardiovascular events.[35] Recent literature has reported that hexokinase mediated G6PD reaction is critical to provide the NADPH reducing equivalents via the PPP for BLVRB cofactor function.[64,65] This may explain the significant association between BLVRB expression and PVI scores, as well as the positive association between glycolysis enzyme protein expression and BLVRB expression in atherosclerotic plaques. Thus, iron loading, as a result of BLVRB in Hb metabolism, may exacerbate the severity of atherosclerosis by inducing inflammation and enhancing glycolysis in macrophages. Therefore, high glycolysis activity may not only be a sign of inflammation, but also an indication of increased Hb metabolism, IPH, and adverse cardiovascular events.

4.5 Limitations

In this study, we assessed plaque vulnerability using the PVI, a semi-quantitative score derived from histological examination. Although this method may seem limited compared with other high-resolution techniques, such as RNA sequencing and untargeted proteomic analysis, it’s important to note that these histological measures have been demonstrated to be reproducible and to correlate with clinical presentation. A notable limitation of our study, however, is the underrepresentation of female patients, constituting only 25% of our sample. This imbalance results in lower statistical power for the female-only dataset. Despite this challenge, we were still able to identify sex-specific signals. Additionally, the selection strategy of patients for proteomics analysis led to the inclusion of patients with slightly higher future risk of MACE compared with the whole cohort.

4.6 Conclusion

The amalgamation of proteomic, transcriptomic, histological, and clinical analysis has revealed 240 ECM proteins significantly linked to PVI scores in human atherosclerotic lesions. The expression of these proteins is substantially affected by multiple histological plaque characteristics, especially plaque macrophage and fat content. Aside from these proteins, we have detected a potential link between glycolysis and plaque vulnerability where three rate-limiting glycolytic enzymes (Hexokinase, PFK, PK) exhibited increased protein expression in more vulnerable plaques. Notably, high expression of these enzymes was detected in inflammatory macrophages, foam cells and SMCs, which may indicate that these cells may be responsible for the observed increased presence of these enzymes. Another notable finding was the significant interaction effect between PVI scores and sex, which suggested that increased expression of these glycolytic enzymes may lead to more profound destabilising effects in female atherosclerotic lesions.

Lastly, LDH, an enzyme involved in the end-stages of glycolysis, was found with significant positive associations with PVI scores. This may be explained by the associated promotion of plaque instability attributed to the induction of acidosis and VSMC phenotypic switching caused by lactate build-up within the plaque. Additionally, a significant association was found between the glycolysis enzymes and the IPH predictive marker BLVRB, which may suggest that the glycolysis process or its end products may participate in plaque instability through multiple pathways, including heme metabolism.

Translational perspective

This study suggests that glycolysis and enzymes like Hexokinase 3 (HK3) are potential therapeutic targets in atherosclerosis, as their increased abundance in vulnerable plaques indicates a role in plaque destabilisation and haemorrhage. Targeting HK3 and other glycolysis-related enzymes may offer new opportunities for treatment by mitigating plaque progression. Additionally, the findings emphasize the importance of integrating multi-omics approaches to better understand atherosclerotic disease, as transcriptomic and proteomic data do not always align.

Supplementary material

Supplementary material is available at *Cardiovascular Research* online.

Acknowledgements

We are thankful for the support of the Dutch Heart Foundation, project TRANS (project 01-003-2022-0417 2022), VAR (TKI-2003), Leducq Fondation 'PlaqOmics' (18CDV-02), EU H2020 TO_AITION (grant number: 848146), EU HORIZON NextGen (grant number: 101136962), and EU HORIZON MIRACLE (grant number: 101115381). The collaborative project 'Getting the Perfect Image' was co-financed through use of PPP Allowance awarded by Health~Holland, Top Sector Life Sciences and Health, to stimulate public-private partnerships. We would like to thank all the (former) employees involved in the Athero-Express Biobank Study of the Departments of Surgery of the St. Antonius Hospital Nieuwegein and University Medical Centre Utrecht for their continuing work. Lastly, we would like to thank all participants of the Athero-Express Biobank Study; without you these kinds of studies would not be possible. We acknowledge bioRender for providing components of the figures.

Conflict of interest: none declared.

Funding

Dr. S.W.v.d.L. is funded through Health~Holland PPP Allowance 'Getting the Perfect Image' and CZI 'MetaPlaq'. Part of this study was funded by the European Union project European Research Council consolidator grant 866478 (UCARE) and the Leducq Foundation AtheroGEN.

Data availability

The data, analytic methods, and study materials will be maintained by the corresponding author and made available to other researchers upon request.

References

1. Nedkoff L, Briffa T, Zemedikun D, Herrington S, Wright FL. Global trends in atherosclerotic cardiovascular disease. *Clin Ther* 2023;**45**:1087–1091.
2. van der Wal AC, Becker AE, van der Loos CM, Tigges AJ, Das PK. Fibrous and lipid-rich atherosclerotic plaques are part of interchangeable morphologies related to inflammation: a concept. *Coron Artery Dis* 1994;**5**:463–469.
3. Libby P. The changing landscape of atherosclerosis. *Nature* 2021;**592**:524–533.
4. Stary HC, Chandler AB, Dinsmore RE, Fuster V, Glagov S, Insull W, Rosenfeld ME, Schwartz CJ, Wagner WD, Wissler RW. A definition of advanced types of atherosclerotic lesions and a histological classification of atherosclerosis. *Circulation* 1995;**92**:1355–1374.
5. Hellings WE, Peeters W, Moll FL, Piers SRD, van Setten J, Van der Spek PJ, de Vries J-PPM, Seldenrijk KA, De Bruin PC, Vink A, Velema E, de Kleijn DPV, Pasterkamp G. Composition of carotid atherosclerotic plaque is associated with cardiovascular outcome. *Circulation* 2010; **121**:1941–1950.
6. Pérez Sorí Y, Herrera Moya VA, Puig Reyes I, Moreno-Martínez FL, Bermúdez Alemán R, Rodríguez Millares T, Fleites Medina A. Histology of atherosclerotic plaque from coronary arteries of deceased patients after coronary artery bypass graft surgery. *Clín Investig Arterioscler* 2019;**31**:63–72.
7. Poznyak AV, Silaeva YY, Orekhov AN, Deykin AV. Animal models of human atherosclerosis: current progress. *Braz J Med Biol Res* 2020;**53**:e9557.
8. Depuydt MAC, Prange KHM, Slenders L, Örd T, Elbersen D, Boltjes A, de Jager SCA, Asselbergs FW, de Borst GJ, Aavik E, Lönnberg T, Lutgens E, Glass CK, den Ruijter HM, Kaikkonen MU, Bot I, Slütter B, van der Laan SW, Yla-Herttuala S, Mokry M, Kuiper J, de Winther MPJ, Pasterkamp G. Microanatomy of the human atherosclerotic plaque by single-cell transcriptomics. *Circ Res* 2020;**127**:1437–1455.
9. Elishaev M, Hodonsky CJ, Ghosh SKB, Finn AV, von Scheidt M, Wang Y. Opportunities and challenges in understanding atherosclerosis by human biospecimen studies. *Front Cardiovasc Med* 2022;**9**:948492.
10. Mokry M, Boltjes A, Slenders L, Bel-Bordes G, Cui K, Brouwer E, Mekke JM, Depuydt MAC, Timmerman N, Waissi F, Verwer MC, Turner AW, Khan MD, Hodonsky CJ, Benavente ED, Hartman RJG, van den Dungen NAM, Lansu N, Nagyova E, Prange KHM, Kovacic JC, Björkegren JLM, Pavlos E, Andreakos E, Schunkert H, Owens GK, Monaco C, Finn AV, Virmani R, Leeper NJ, de Winther MPJ, Kuiper J, de Borst GJ, Stroes ESG, Civelek M, de Kleijn DPV, den Ruijter HM, Asselbergs FW, van der Laan SW, Miller CL, Pasterkamp G. Transcriptomic-based clustering of human atherosclerotic plaques identifies subgroups with different underlying biology and clinical presentation. *Nat Cardiovasc Res* 2022;**1**: 1140–1155.
11. Satam H, Joshi K, Mangrolia U, Waghoo S, Zaidi G, Rawool S, Thakare RP, Banday S, Mishra AK, Das G, Malonia SK. Next-generation sequencing technology: current trends and advancements. *Biology (Basel)* 2023;**12**:997.
12. Edfors F, Danielsson F, Hallström BM, Käll L, Lundberg E, Pontén F, Forsström B, Uhlén M. Gene-specific correlation of RNA and protein levels in human cells and tissues. *Mol Syst Biol* 2016;**12**:883.
13. Liu Y, Beyer A, Aebersold R. On the dependency of cellular protein levels on mRNA abundance. *Cell* 2016;**165**:535–550.
14. Verhoeven B, Hellings WE, Moll FL, de Vries JP, de Kleijn DPV, de Bruin P, Busser E, Schoneveld AH, Pasterkamp G. Carotid atherosclerotic plaques in patients with transient ischemic attacks and stroke have unstable characteristics compared with plaques in asymptomatic and amaurosis fugax patients. *J Vasc Surg* 2005;**42**:1075–1081.
15. Ferguson GG, Eliasziw M, Barr HWK, Clagett GP, Barnes RW, Wallace MC, Taylor DW, Haynes RB, Finan JW, Hachinski VC, Barnett HJM. The North American symptomatic carotid endarterectomy trial: surgical results in 1415 patients. *Stroke* 1999;**30**:1751–1758.
16. Lusby RJ, Ferrell LD, Ehrenfeld WK, Stoney RJ, Wylie EJ. Carotid plaque hemorrhage. Its role in production of cerebral ischemia. *Arch Surg* 1982;**117**:1479–1488.
17. Schwartz SM, Galis ZS, Rosenfeld ME, Falk E. Plaque rupture in humans and mice. *Arterioscler Thromb Vasc Biol* 2007;**27**:705–713.
18. Ménégaut L, Jalil A, Pilot T, van Dongen K, Crespy V, Steinmetz E, Pais de Barros JP, Geissler A, Le Goff W, Venteclef N, Lagrost L, Gautier T, Thomas C, Masson D. Regulation of glycolytic genes in human macrophages by oxysterols: a potential role for liver X receptors. *Br J Pharmacol* 2021;**178**:3124–3139.
19. Ionita MG, van den Borne P, Catanzariti LM, Moll FL, de Vries J-PPM, Pasterkamp G, Vink A, de Kleijn DPV. High neutrophil numbers in human carotid atherosclerotic plaques are associated with characteristics of rupture-prone lesions. *Arterioscler Thromb Vasc Biol* 2010;**30**: 1842–1848.
20. Mekke JM, Egberts DHJ, Waissi F, Timmerman N, Bot I, Kuiper J, Pasterkamp G, de Borst GJ, de Kleijn DPV. Mast cell distribution in human carotid atherosclerotic plaque differs significantly by histological segment. *Eur J Vasc Endovasc Surg* 2021;**62**:808–815.
21. Willems S, Vink A, Bot I, Quax PHA, de Borst GJ, de Vries J-PPM, van de Weg SM, Moll FL, Kuiper J, Kovanen PT, de Kleijn DPV, Hoefer IE, Pasterkamp G. Mast cells in human carotid atherosclerotic plaques are associated with intraplaque microvessel density and the occurrence of future cardiovascular events. *Eur Heart J* 2013;**34**:3699–3706.

22. Slenders L, Landsmeer LPL, Cui K, Depuydt MAC, Verwer M, Mekke J, Timmerman N, van den Dungen NAM, Kuiper J, de Winther MPJ, Prange KHM, Ma WF, Miller CL, Aherrahrou R, Civelek M, de Borst GJ, de Kleijn DPV, Asselbergs FW, den Ruijter HM, Boltjes A, Pasterkamp G, van der Laan SW, Mokry M. Intersecting single-cell transcriptomics and genome-wide association studies identifies crucial cell populations and candidate genes for atherosclerosis. *Eur Heart J Open* 2022;**2**:oeab043.
23. Diez Benavente E, Karnewar S, Buono M, Mili E, Hartman RJG, Kapteijn D, Slenders L, Daniels M, Aherrahrou R, Reinberger T, Mol BM, de Borst GJ, de Kleijn DPV, Prange KHM, Depuydt MAC, de Winther MPJ, Kuiper J, Björkegren JLM, Erdmann J, Civelek M, Mokry M, Owens GK, Pasterkamp G, den Ruijter HM. Female gene networks are expressed in myofibroblast-like smooth muscle cells in vulnerable atherosclerotic plaques. *Arterioscler Thromb Vasc Biol* 2023;**43**:1836–1850.
24. Jin H, Goossens P, Juhasz P, Eijgelaar W, Manca M, Karel JMH, Smirnov E, Sikkink CJJM, Mees BME, Waring O, van Kuijk K, Fazzi GE, Gijbels MJJ, Kutmon M, Evelo CTA, Hedin U, Daemen MJAP, Sluimer JC, Matic L, Biessen EAL. Integrative multiomics analysis of human atherosclerosis reveals a serum response factor-driven network associated with intraplaque hemorrhage. *Clin Transl Med* 2021;**11**:e458.
25. Kuleshov MV, Jones MR, Rouillard AD, Fernandez NF, Duan Q, Wang Z, Koplev S, Jenkins SL, Jagodnik KM, Lachmann A, McDermott MG, Monteiro CD, Gundersen GW, Ma'ayan A. Enrichr: a comprehensive gene set enrichment analysis web server 2016 update. *Nucleic Acids Res* 2016;**44**:W90–W97.
26. Wu T, Hu E, Xu S, Chen M, Guo P, Dai Z, Feng T, Zhou L, Tang W, Zhan L, Fu X, Liu S, Bo X, Yu G. clusterProfiler 4.0: a universal enrichment tool for interpreting omics data. *Innovation* 2021;**2**:100141.
27. Cleland NRW, Al-Juboori SI, Dobrinskikh E, Bruce KD. Altered substrate metabolism in neurodegenerative disease: new insights from metabolic imaging. *J Neuroinflammation* 2021;**18**:248.
28. Wu W, Zhao S. Metabolic changes in cancer: beyond the Warburg effect. *Acta Biochim Biophys Sin (Shanghai)* 2013;**45**:18–26.
29. Li L, Wang M, Ma Q, Ye J, Sun G. Role of glycolysis in the development of atherosclerosis. *Am J Physiol Cell Physiol* 2022;**323**:C617–C629.
30. Li X-B, Gu J-D, Zhou Q-H. Review of aerobic glycolysis and its key enzymes—new targets for lung cancer therapy. *Thorac Cancer* 2015;**6**:17–24.
31. Yang P, Xu W, Liu L, Yang G. Association of lactate dehydrogenase and diabetic retinopathy in US adults with diabetes mellitus. *Journal of Diabetes* 2023;**16**. https://doi.org/10.1111/1753-0407.13476
32. Mishra D, Banerjee D. Lactate dehydrogenases as metabolic links between tumor and stroma in the tumor microenvironment. *Cancers (Basel)* 2019;**11**:750.
33. Poznyak A, Grechko AV, Poggio P, Myasoedova VA, Alfieri V, Orekhov AN. The diabetes mellitus–atherosclerosis connection: the role of lipid and glucose metabolism and chronic inflammation. *Int J Mol Sci* 2020;**21**:1835.
34. Theofilatos K, Stojkovic S, Hasman M, van der Laan SW, Baig F, Barallobre-Barreiro J, Schmidt LE, Yin S, Yin X, Burnap S, Singh B, Popham J, Harkot O, Kampf S, Nackenhorst MC, Strassl A, Loewe C, Demyanets S, Neumayer C, Bilban M, Hengstenberg C, Huber K, Pasterkamp G, Wojta J, Mayr M. Proteomic atlas of atherosclerosis: the contribution of proteoglycans to sex differences, plaque phenotypes, and outcomes. *Circ Res* 2023;**133**:542–558.
35. Chemaly M, Marlevi D, Iglesias M-J, Lengquist M, Kronqvist M, Bos D, van Dam-Nolen DHK, van der Kolk A, Hendrikse J, Kassem M, Matic L, Odeberg J, de Vries MR, Kooi ME, Hedin U. Biliverdin reductase B is a plasma biomarker for intraplaque hemorrhage and a predictor of ischemic stroke in patients with symptomatic carotid atherosclerosis. *Biomolecules* 2023;**13**:882.
36. Matic LP, Jesus Iglesias M, Vesterlund M, Lengquist M, Hong M-G, Saieed S, Sanchez-Rivera L, Berg M, Razuvaev A, Kronqvist M, Lund K, Caidahl K, Gillgren P, Pontén F, Uhlén M, Schwenk JM, Hansson GK, Paulsson-Berne G, Fagman E, Roy J, Hultgren R, Bergström G, Lehtiö J, Odeberg J, Hedin U. Novel multiomics profiling of human carotid atherosclerotic plaques and plasma reveals biliverdin reductase B as a marker of intraplaque hemorrhage. *JACC Basic Transl Sci* 2018;**3**:464–480.
37. van Dam-Nolen DHK, van Egmond NCM, Koudstaal PJ, van der Lugt A, Bos D. Sex differences in carotid atherosclerosis: a systematic review and meta-analysis. *Stroke* 2023;**54**:315–326.
38. Fairweather D. Sex differences in inflammation during atherosclerosis. *Clin Med Insights Cardiol* 2015;**8**:49–59.
39. Hazzard WR. Atherogenesis: why women live longer than men. *Geriatrics* 1985;**40**:42–51, 54.
40. Legato MJ. Dyslipidemia, gender, and the role of high-density lipoprotein cholesterol: implications for therapy. *Am J Cardiol* 2000;**86**:15–18.
41. Xiao Q, Hou R, Xie L, Niu M, Pan X, Zhu X. Macrophage metabolic reprogramming and atherosclerotic plaque microenvironment: fostering each other? *Clin Transl Med* 2023;**13**:e1257.
42. Sopić M, Karaduzovic-Hadziabdic K, Kardassis D, Maegdefessel L, Martelli F, Meerson A, Munjas J, Niculescu LS, Stoll M, Magni P, Devaux Y. Transcriptomic research in atherosclerosis: unravelling plaque phenotype and overcoming methodological challenges. *J Mol Cell Cardiol Plus* 2023;**6**:100048.
43. Mathieson T, Franken H, Kosinski J, Kurzawa N, Zinn N, Sweetman G, Poeckel D, Ratnu VS, Schramm M, Becher I, Steidel M, Noh K-M, Bergamini G, Beck M, Bantscheff M, Savitski MM. Systematic analysis of protein turnover in primary cells. *Nat Commun* 2018;**9**:689.
44. Wang C, Liu H. Factors influencing degradation kinetics of mRNAs and half-lives of microRNAs, circRNAs, lncRNAs in blood in vitro using quantitative PCR. *Sci Rep* 2022;**12**:7259.
45. Bot PT, Grundmann S, Goumans M-J, de Kleijn D, Moll F, de Boer O, van der Wal AC, van Soest A, de Vries J-P, van Royen N, Piek JJ, Pasterkamp G, Hoefer IE. Forkhead box protein P1 as a downstream target of transforming growth factor-β induces collagen synthesis and correlates with a more stable plaque phenotype. *Atherosclerosis* 2011;**218**:33–43.
46. Peeters W, de Kleijn DPV, Vink A, van de Weg S, Schoneveld AH, Sze SK, van der Spek PJ, de Vries J-PPM, Moll FL, Pasterkamp G. Adipocyte fatty acid binding protein in atherosclerotic plaques is associated with local vulnerability and is predictive for the occurrence of adverse cardiovascular events. *Eur Heart J* 2011;**32**:1758–1768.
47. Boyalla V, Gallego-Colon E, Spartalis M. Immunity and inflammation in cardiovascular disorders. *BMC Cardiovasc Disord* 2023;**23**:148.
48. Galkina E, Ley K. Immune and inflammatory mechanisms of atherosclerosis. *Annu Rev Immunol* 2009;**27**:165–197.
49. Kong P, Cui Z-Y, Huang X-F, Zhang D-D, Guo R-J, Han M. Inflammation and atherosclerosis: signaling pathways and therapeutic intervention. *Signal Transduct Target Ther* 2022;**7**:131.
50. Maedler K, Sergeev P, Ris F, Oberholzer J, Joller-Jemelka HI, Spinas GA, Kaiser N, Halban PA, Donath MY. Glucose-induced β cell production of IL-1β contributes to glucotoxicity in human pancreatic islets. *J Clin Invest* 2017;**127**:1589.
51. Xu R, Yuan W, Wang Z. Advances in glycolysis metabolism of atherosclerosis. *J Cardiovasc Transl Res* 2023;**16**:476–490.
52. Vrieling F, van Dierendonck XAMH, Jaeger M, Janssen AWM, Hijmans A, Netea MG, Tack CJ, Stienstra R. Glycolytic activity in human immune cells: inter-individual variation and functional implications during health and diabetes. *Immunometabolism (Cobham)* 2022;**4**:e00008.
53. Bories GFP, Leitinger N. Macrophage metabolism in atherosclerosis. *FEBS Lett* 2017;**591**:3042–3060.
54. Chen H, Yang J, Zhang Q, Chen L-H, Wang Q. Corosolic acid ameliorates atherosclerosis in apolipoprotein E-deficient mice by regulating the nuclear factor-κB signaling pathway and inhibiting monocyte chemoattractant protein-1 expression. *Circ J* 2012;**76**:995–1003.
55. Zhang W, Zhao E, Li Z, Liu W, Wang J, Hou W, Zhang N, Yu Y, Li X, You B. Hexokinase HK3-mediated O-GlcNAcylation of EP300: a key regulator of PD-L1 expression and immune evasion in ccRCC. *Cell Death Dis* 2024;**15**:613.
56. Heiss EH, Schachner D, Donati M, Grojer CS, Dirsch VM. Increased aerobic glycolysis is important for the motility of activated VSMC and inhibited by indirubin-3′-monoxime. *Vascul Pharmacol* 2016;**83**:47–56.
57. Yang L, Gao L, Nickel T, Yang J, Zhou J, Gilbertsen A, Geng Z, Johnson C, Young B, Henke C, Gourley GR, Zhang J. Lactate promotes synthetic phenotype in vascular smooth muscle cells. *Circ Res* 2017;**121**:1251–1262.
58. Shantha GPS, Wasserman B, Astor BC, Coresh J, Brancati F, Sharrett AR, Young JH. Association of blood lactate with carotid atherosclerosis: the Atherosclerosis Risk in Communities (ARIC) Carotid MRI Study. *Atherosclerosis* 2013;**228**:249–255.
59. Jain M, Dhanesha N, Doddapattar P, Nayak MK, Guo L, Cornelissen A, Lentz SR, Finn AV, Chauhan AK. Smooth muscle cell specific pyruvate kinase M2 promotes SMC phenotypic switching and neointimal hyperplasia. *Arterioscler Thromb Vasc Biol* 2021;**41**:1724–1737.
60. Seeley EH, Liu Z, Yuan S, Stroope C, Cockerham E, Rashdan NA, Delgadillo LF, Finney AC, Kumar D, Das S, Razani B, Liu W, Traylor J, Orr AW, Rom O, Pattillo CB, Yurdagul A. Spatially resolved metabolites in stable and unstable human atherosclerotic plaques identified by mass spectrometry imaging. *Arterioscler Thromb Vasc Biol* 2023;**43**:1626–1635.
61. Hellings WE, Pasterkamp G, Verhoeven BAN, De Kleijn DPV, De Vries J-PPM, Seldenrijk KA, van den Broek T, Moll FL. Gender-associated differences in plaque phenotype of patients undergoing carotid endarterectomy. *J Vasc Surg* 2007;**45**:289–296; discussion 296–297.
62. Hartman RJG, Owsiany K, Ma L, Koplev S, Hao K, Slenders L, Civelek M, Mokry M, Kovacic JC, Pasterkamp G, Owens G, Björkegren JLM, den Ruijter HM. Sex-stratified gene regulatory networks reveal female key driver genes of atherosclerosis involved in smooth muscle cell phenotype switching. *Circulation* 2021;**143**:713–726.
63. Newman AAC, Serbulea V, Baylis RA, Shankman LS, Bradley X, Alencar GF, Owsiany K, Deaton RA, Karnewar S, Shamsuzzaman S, Salamon A, Reddy MS, Guo L, Finn A, Virmani R, Cherepanova OA, Owens GK. Multiple cell types contribute to the atherosclerotic lesion fibrous cap by PDGFRβ and bioenergetic mechanisms. *Nat Metab* 2021;**3**:166–181.
64. Bahou WF, Marchenko N, Nesbitt NM. Metabolic functions of biliverdin IXβ reductase in redox-regulated hematopoietic cell fate. *Antioxidants* 2023;**12**:1058.
65. Li Z, Nesbitt NM, Malone LE, Gnatenko DV, Wu S, Wang D, Zhu W, Girnun GD, Bahou WF. Heme degradation enzyme biliverdin IXβ reductase is required for stem cell glutamine metabolism. *Biochem J* 2018;**475**:1211–1223.